

"In presenting the dissertation as a partial fulfillment of the requirements for an advanced degree from the Georgia Institute of Technology, I agree that the Library of the Institution shall make it available for inspection and circulation in accordance with its regulations governing materials of this type. I agree that permission to copy from, or to publish from, this dissertation may be granted by the professor under whose direction it was written, or, in his absence, by the dean of the Graduate Division when such copying or publication is solely for scholarly purposes and does not involve potential financial gain. It is understood that any copying from, or publication of, this dissertation which involves potential financial gain will not be allowed without written permission.

---

INVESTIGATION OF A CARRIER CANCELLATION TECHNIQUE FOR EXTENDING  
THE DYNAMIC RANGE OF SPECTRUM ANALYZERS

A THESIS

Presented to

the Faculty of the Graduate Division

by

John Gerald Holey

In Partial Fulfillment

of the Requirements for the Degree

Master of Science in Electrical Engineering

Georgia Institute of Technology

May, 1962

42  
12 R

INVESTIGATION OF A CARRIER CANCELLATION TECHNIQUE FOR EXTENDING  
THE DYNAMIC RANGE OF SPECTRUM ANALYZERS

Approved:

*[Handwritten signature]*  
\_\_\_\_\_  
\_\_\_\_\_

Date approved by Chairman May 31, 19

## PREFACE

This study was conducted with the primary purpose of developing an improved technique for measurement of radiation characteristics of radio-frequency transmitters. It is hoped that the technique presented will prove useful for future investigations into this relatively unknown area.

The author wishes to express thanks to Dr. J. L. Hammond for his assistance and advice, to Dr. D. L. Finn and Mr. C. E. Blakely for their suggestions, to Mrs. B. S. Queary for her assistance in preparation of the manuscript, and to Mr. R. N. Bailey for his patience and advice.

A large portion of the experimental work conducted in this investigation was done in connection with Department of the Army Contract No. DA-36-039-sc-87183.

## TABLE OF CONTENTS

	Page
PREFACE. . . . .	ii
LIST OF FIGURES. . . . .	v
SUMMARY. . . . .	viii
Chapter	
I. INTRODUCTION . . . . .	1
II. EFFECTS OF A STRONG CARRIER. . . . .	9
III. CARRIER REDUCTION TECHNIQUES . . . . .	14
Passive Filter Networks	
Active Filter Networks	
IV. DESIGN REQUIREMENTS FOR CARRIER CANCELLATION DEVICE. . . .	18
Introduction	
Amplifiers	
Cathode Follower	
Delay Line	
V. EXPERIMENTAL RESULTS . . . . .	41
Frequency Response Characteristics of Single Amplifier	
Stage	
Frequency Response of Three Cascaded Cancellation,	
Tone-Modulated Input Signal	
Response of Device with Carrier Cancellation,	
Noise-Modulated Input Signal	
Noise Level of Device	
Noise and Distortion of Typical AM Transmitter	
VI. CONCLUSIONS AND RECOMMENDATIONS. . . . .	58
APPENDIX	
A. Computer Program for Calculating Selectivity of Bandpass	
Amplifiers . . . . .	62

## TABLE OF CONTENTS (Continued)

	Page
B. Bridged-T Filter Design. . . . .	67
C. Schematic Diagram of Carrier Cancellation Device . . . . .	69
BIBLIOGRAPHY. . . . .	70

## LIST OF FIGURES

	Page
1. Frequency Spectrum of AM Transmitter Showing Distortion Sidebands. . . . .	4
2. Block Diagram of Distortion Analyzer . . . . .	6
3. Block Diagram of Spectrum Analyzer . . . . .	7
4. Frequency Spectrum of Single-Sideband Signal Without Intermodulation (A) and with Intermodulation (B). . . . .	11
5. Schematic Diagram of Typical Bridged-T Network . . . . .	15
6. Block Diagram of Carrier Cancellation Device . . . . .	17
7. Equivalent Circuit of Plate Load . . . . .	19
8. Reduction of Equivalent Circuit. . . . .	23
9. Test Setup for Measuring Q of Toroidal Inductors . . . . .	27
10. Frequency Response of Five Toroidal Inductances . . . . .	29
11. Q Versus Frequency For Toroidal Inductance . . . . .	30
12. Schematic Diagram of Amplifier Stage . . . . .	32
13. A-C Equivalent Circuit of Amplifier Stage. . . . .	34
14. Schematic Diagram of Cathode Follower Circuit. . . . .	36
15. Section of Delay Line. . . . .	38
16. Test Setup for Measuring Frequency Response of Single Amplifier Stage. . . . .	42
17. Frequency Response of Single Amplifier Stage . . . . .	43
18. Display of Power Density Spectrum of Output of Single Amplifier Stage. Signal Modulated 10% by 500 Kc Random Noise. . . . .	44
19. Display of Power Density Spectrum of Input to Amplifier Stage in Figure 17 . . . . .	44

## LIST OF FIGURES (Continued)

	Page
20. Frequency Response of Three-Stage Amplifier. . . . .	46
21. Display of Power Density Spectrum of Output of Three Cascaded Amplifier Stages. Signal Modulated 10% by 500 Kc Random Noise .	47
22. Setup for Measuring Amplifier Bandwidth Using Sweep Generator. .	48
23. Frequency Characteristics of Three Cascaded Amplifier Stages Using Sweep Generator. . . . .	49
24. Display of Output Power Density Spectrum of Cancellation Device Without Carrier Cancellation. Input Signal Unmodulated. . . . .	51
25. Display of Output Power Density Spectrum of Cancellation Device with 40 db Carrier Cancellation. Input Signal Unmodulated . . .	51
26. Display of Output Power Density Spectrum of Cancellation Device Without Cancellation. Input Signal Modulated 10% by 10 Kc Tone.	51
27. Display of Output Power Density Spectrum of Cancellation Device with 40 db Carrier Cancellation. Input Signal Modulated 10% by 10 Kc Tone. . . . .	51
28. Display of Output Power Density Spectrum of Cancellation Device without Carrier Cancellation. Input Signal Modulated 10% By 15 Kc Tone. Carrier and Lower Sideband . . . . .	52
29. Display of Output Power Density Spectrum of Cancellation Device with 40 Db Carrier Cancellation. Input Signal Modulated 10% By 15 Kc Tone. Carrier and Lower Sideband. . . . .	52
30. Display of Output Power Density Spectrum of Cancellation Device Without Carrier Cancellation. Input Signal Modulated 10% By 15 Kc Tone. Carrier and Upper Sideband . . . . .	52
31. Display of Output Power Density Spectrum of Cancellation Device With 40 Db Carrier Cancellation. Input Signal Modulated 10% by 15 Kc Tone. Carrier and Upper Sideband . . . . .	52
32. Frequency Response of Overall Circuitry. . . . .	53
33. Display of Output Power Density Spectrum of Cancellation Device With 40 Db Carrier Cancellation. Input Signal Modulated 10% By 500 Kc Random Noise . . . . .	55

## LIST OF FIGURES (Continued)

	Page
34. Display of Output Power Density Spectrum of Cancellation Device Without Carrier Cancellation. Input Signal Modulated 10% By 500 Kc Random Noise . . . . .	55
35. Display of Output Power Density Spectrum of Cancellation Device Showing Residual Noise with No Input Signal . . . . .	55
36. Display of Spectrum Analyzer with No Input To Spectrum Analyzer .	55
37. Display of Output Power Density Spectrum of Cancellation Device Without Carrier Cancellation. Input Signal From Test Transmitter Modulated 100% by 3 Kc Tone. Visible Distortion Products Extend to 60 db Below Carrier . . . . .	57
38. Display of Output Power Density Spectrum of Cancellation Device with 30 Db Carrier Cancellation. Input Signal From Test Transmitter Modulated 100% by 3 Kc Tone. Visible Distortion Products Extend to 80 db Below Carrier . . . . .	57
39. Display of Output Power Density Spectrum of Cancellation Device Without Carrier Cancellation. Input Signal From Unmodulated Test Transmitter. Noise Components Not Visible . . . . .	57
40. Display of Output Power Density Spectrum of Cancellation Device with 40 Db Carrier Cancellation. Input Signal From Unmodulated Test Transmitter. Noise Components Visible 75 Db Below Carrier	57
41. Photograph of Carrier Cancellation Device . . . . .	59
1B. Frequency Response of Bridged "T" Filter. . . . .	68

## SUMMARY

The purpose of this investigation was to determine the effectiveness of a method of extending the range of commercial spectrum analyzers, from the present 60 db, to 80 db through the use of an active carrier cancellation device.

It had been previously observed that noise spectral components of the output power density spectrum of amplitude-modulated transmitters were generally more than 60 db below the amplitude of the carrier, and examination of these components through the use of spectrum analyzers was not possible without the use of elaborate mechanical or crystal passive filter networks.

A device was successfully constructed and tested using the carrier cancellation method. By selectively amplifying the carrier component of the power density spectrum, altering the phase of this component by 180 degrees, and combining it with the original signal, the amplitude of the carrier was consistently reduced by 30 to 40 db, regardless of the characteristics of the power density spectrum of the signal under test. The selectivity of the device was considerably greater than other passive L-C networks in current use, notably the bridged-T rejection network.

It was concluded that the approach for extending the dynamic range of spectrum analyzers that was developed in the thesis provides a significant addition to present laboratory test methods for determining

transmitter characteristics. The method investigated may, in addition, prove to be of considerable value in such future studies as the analysis and determination of the randomness of residual noise spectral components contained in the output power density spectrum of a transmitter.

It was recommended that the device be modified through the addition of bandpass amplifier stages to determine the practical limit in selectivity characteristics of the carrier cancellation device.

## CHAPTER I

## INTRODUCTION

A common source of interference in communications systems is a transmitter producing radio-frequency outputs at frequencies other than the fundamental frequency. For example, a transmitter operating at a particular assigned frequency will, in addition, be radiating energy at integral multiples, or harmonics, of the operating frequency. Output energy may also be present that is due to various oscillators, etc., within the transmitter. In addition to these discrete frequencies which are related in some manner to oscillators within the transmitter, the transmitter carrier is often modulated by extraneous random noise, or the transmitter may suffer oscillator-frequency perturbations which cause noise sidebands. Also, nonlinearities in the transmitter may result in undesired frequency spectrum components. It is important in many installations that both the frequency and amplitude of each of these "spurious" or undesired emissions be known, in order to preclude interference with receivers operating in the vicinity of the transmitter. Thus, the power density spectrum of the output carrier under both modulated and unmodulated conditions is frequently useful.

To illustrate interference resulting from nonlinearities existing within the transmitter circuitry, consider that an audio frequency modulating voltage,

$$e_m(t) = E_m \cos \omega_m t, \quad (1)$$

where  $E_m$  is the peak-to-peak voltage and  $\omega_m$  is the frequency of the modulating voltage in radians per second, is applied to the modulator of an amplitude - modulation transmitter. Let the carrier voltage be given by

$$e_c(t) = E_c \cos \omega_c t, \quad (2)$$

where  $E_c$  is the peak-to-peak voltage and  $\omega_c$  is the carrier frequency. Now, the amplitude modulation process can be described mathematically by

$$e_o(t) = E_c [1 + mf(t)] \cos \omega_c t, \quad (3)$$

where  $E_c$  = unmodulated carrier amplitude,

$f(t)$  = modulating voltage,

$m$  = modulation index, or  $E_m/E_c$ ,

$\omega_c$  = carrier frequency in radians per second,

and  $e_o(t)$  = modulated output voltage.

If the modulating voltage  $f(t)$  is represented by  $e_m$  as given in Equation (1), then (3) can be written

$$\begin{aligned} e_o(t) &= E_c [1 + m \cos \omega_m t] \cos \omega_c t & (4) \\ &= E_c \cos \omega_c t + \frac{mE_c}{2} \cos (\omega_c + \omega_m)t \\ &\quad - \frac{mE_c}{2} \cos (\omega_c - \omega_m)t. \end{aligned}$$

It can be seen that if the modulating sinusoid becomes distorted by a nonlinearity within the transmitter, the resulting waveform can be represented by a Fourier Series containing the fundamental frequency

$\omega_m$  and its harmonics, and the modulated wave is given by

$$\begin{aligned}
 e_o(t) = & E_c \cos \omega_c t + E_1 \cos (\omega_c + \omega_m)t - E_1 \cos (\omega_c - \omega_m)t + \\
 & E_2 \cos (\omega_c + 2\omega_m)t - E_2 \cos (\omega_c - 2\omega_m)t + \\
 & E_3 \cos (\omega_c + 3\omega_m)t - E_3 \cos (\omega_c - 3\omega_m)t + \dots .
 \end{aligned} \tag{5}$$

A spectrum of the type described by Equation (5) is given in Figure 1.

The passband of a modulator stage in a communications transmitter is usually three kilocycles, and the assigned channel width ten kilocycles. Thus, from Equation (5) it is clear that harmonics of the modulating frequency can cause the actual spectrum of the transmitted signal to extend into the adjacent channels, thereby causing interference.

In addition to the undesired modulation products, an examination of an unmodulated carrier will reveal random noise sidebands extending considerably beyond the assigned channel frequency limits. These sidebands originate from two sources, namely thermal and tube noise originating in the early stages of the modulator section, and random amplitude and frequency fluctuations of the transmitter oscillator output signal.

Therefore, to completely define the characteristics of a transmitter, this "out-of-channel" radiation should be accurately determined. There are presently several methods in use for measuring the characteristics of a transmitter. Lund<sup>1</sup> describes three methods of measuring adjacent-channel radiation from a transmitter having four voice channels frequency-multiplexed with two channels per sideband. The methods out-

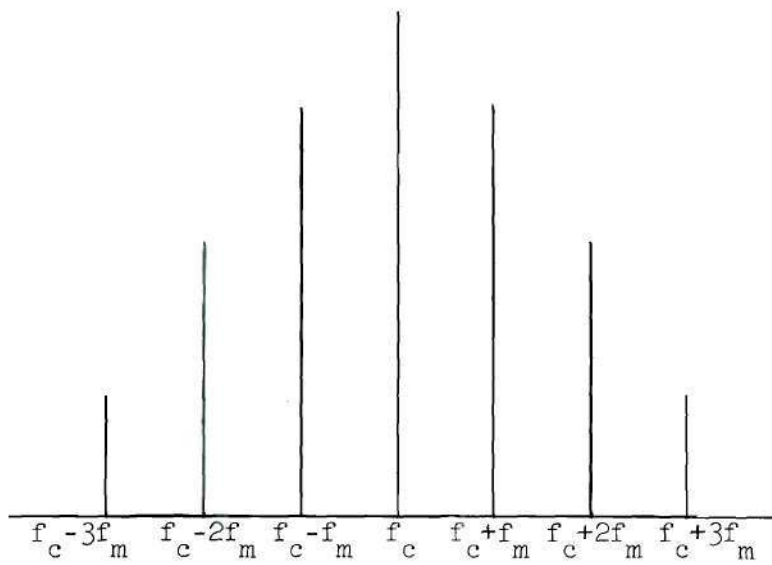


Figure 1. Frequency Spectrum of AM Transmitter Showing Distortion Side-Bands.

lined require full modulation of the transmitter with either two equal tones, normal modulating signals, or thermal noise. The measurements are made by tuning a single-sideband receiver to spot frequencies outside the assigned channel at three-kilocycle intervals. The principal disadvantage of this method is the necessity of a single-sideband receiver to detect the power density spectrum with sufficient selectivity.

The method in common usage for commercial broadcast transmitter measurements is based on the use of a distortion analyzer.<sup>2</sup> A block diagram of a typical distortion analyzer is shown in Figure 2. In this method, the transmitter is modulated with a single audio frequency and the resulting RF signal applied to the terminals of the distortion analyzer. The modulating envelope is then detected and passed through a narrow band rejection network which removes the fundamental audio tone; the remaining harmonics and noise are then measured collectively. This method does not yield any frequency information about the unwanted modulation.

A third method involves the use of a narrow bandpass filter or "window" which is progressively tuned through the frequencies of interest, while recording the output voltage. This method requires an elaborate outlay of filters and is generally considered impractical.

The fourth method is the most commonly used and is the subject of this thesis. This method makes use of a device known as a "spectrum analyzer" to provide an actual visual display of the power density spectrum about the carrier frequency. A block diagram of a typical spectrum analyzer is given in Figure 3.

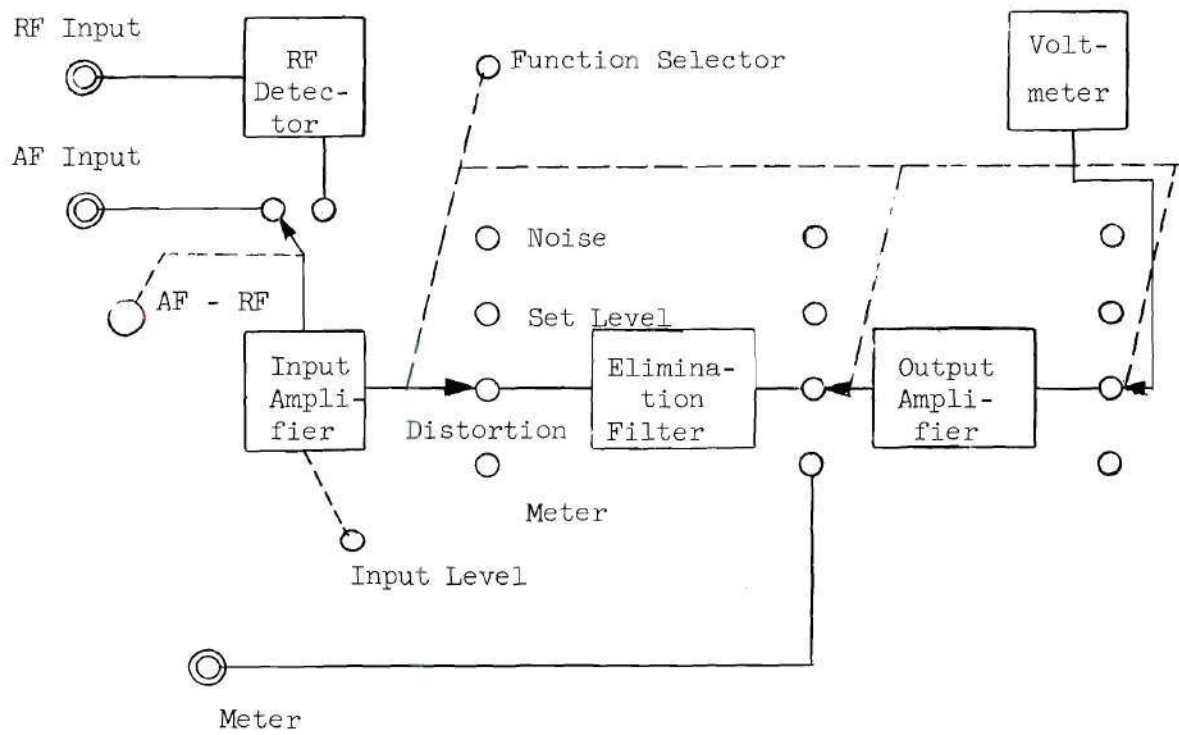


Figure 2. Block Diagram of Distortion Analyzer.

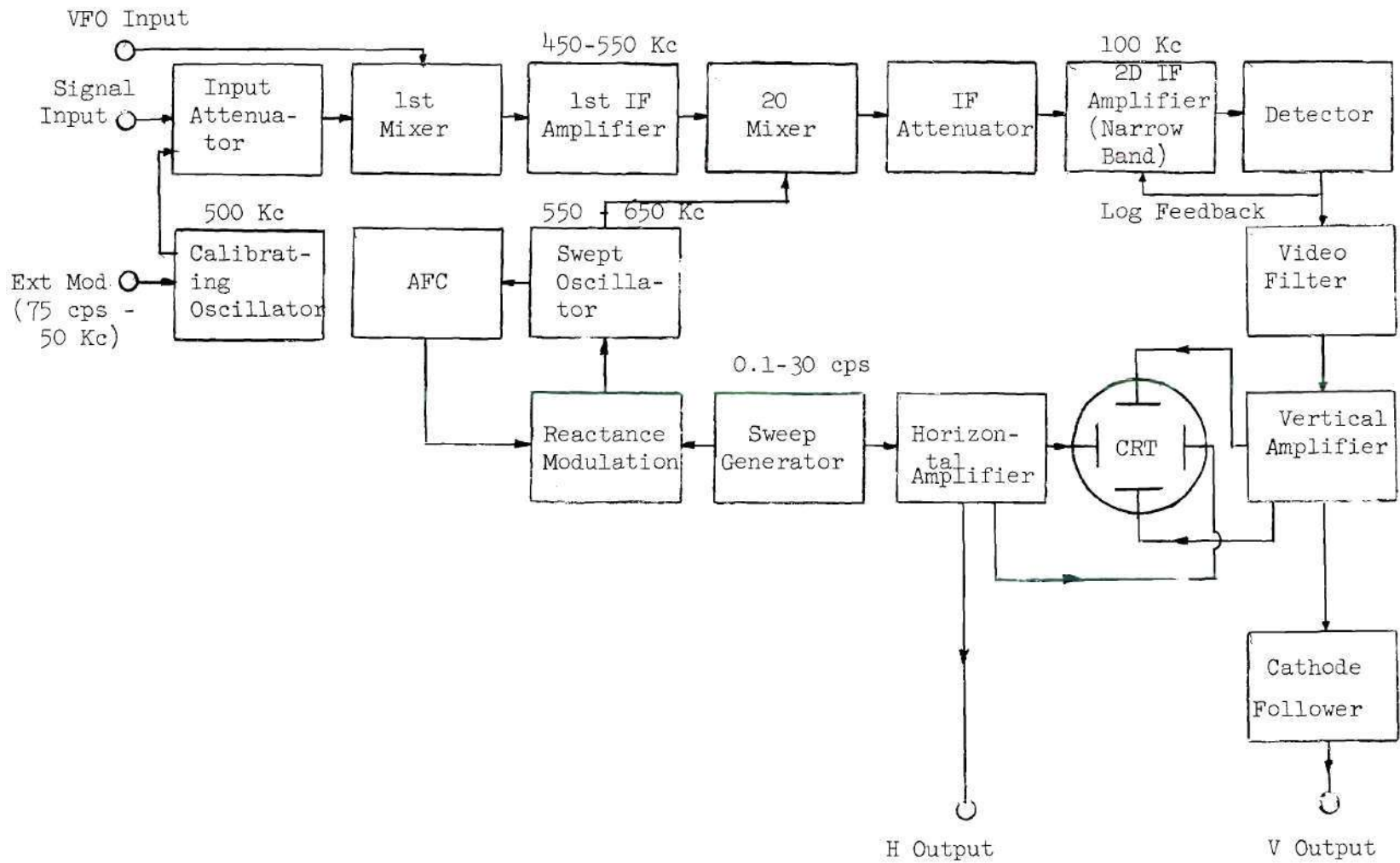


Figure 3. Block Diagram of Spectrum Analyzer

The spectrum analyzer is essentially a receiver with a cathode-ray tube (CRT) as the output device or indicator. The local oscillator is varied in frequency, in synchronism with the sawtooth sweep voltage of the CRT, and produces an intermediate frequency when mixed with the input signal. This signal is passed through a narrow-band filter, detected, and applied to the vertical amplifier of the CRT circuitry. Thus, as the local oscillator sweeps its frequency range, any input signal which will produce the intermediate frequency will appear at the proper time on the CRT sweep. The spectrum analyzer illustrated in Figure 3 will display a spectrum of 100 kilocycles.

## CHAPTER II

## EFFECTS OF A STRONG CARRIER

When a strong carrier signal is applied to the spectrum analyzer, several undesired effects may occur that adversely affect measurements. The first effect to be considered is the susceptibility of the spectrum analyzer to frequencies other than the intended carrier. This effect produces "spurious responses" of the spectrum analyzer, and is described by the equation

$$f_{SR} = \left| \frac{p \cdot f_{LO} \pm f_{IF}}{q} \right| \quad (6)$$

where  $p$  represents harmonics of the local oscillator frequency,  $f_{LO}$ ,  $q$  represents harmonics of the input frequency,  $f_{SR}$ , and  $f_{IF}$  is the intermediate frequency of the spectrum analyzer.

Equation (6) is derived using the fact that an undesired signal,  $f_{SR}$ , or its harmonics,  $q f_{SR}$ , may combine in the mixer stage with the local oscillator signal,  $f_{LO}$ , or its harmonics,  $p f_{LO}$ , to produce the intermediate frequency of the spectrum analyzer,  $f_{IF}$ , and thus cause a response on the display. For instance, if the local oscillator is operated at a frequency which is above the test or desired frequency by an amount equal to  $f_{IF}$ , then the spectrum analyzer will also respond to an unwanted signal the frequency of which is above the local oscillator by an amount equal to  $f_{IF}$ . The frequency of such a spurious signal is

known as the "image" of the spectrum analyzer. In addition to the image, responses may occur as a result of various combinations of harmonics of the local oscillator and test signals according to Equation (6).

The second effect of a strong carrier is intermodulation. This is caused by nonlinearities in the spectrum analyzer, predominately in the mixer stage. Consider an input test signal, for example, of a single sideband transmitter, having two components, the carrier and one sideband removed from the carrier by an amount equal to the frequency of the modulating audio signal. Figure 4(A) shows the power density spectrum of such a signal. This case can be described mathematically by

$$e_i = e_1 \cos \omega_c t + e_2 \cos (\omega_c + \omega_m)t, \quad (7)$$

where  $\omega_c$  and  $\omega_m$  are the carrier and modulation frequencies respectively.

The spectrum analyzer mixer stage can be approximated by the equation

$$e_o = k_1 e_i + k_2 e_i^2 + k_3 e_i^3 + \dots \quad (8)$$

If this equation is expanded through the cubic term, a finite series of terms will result. Two of these terms, which are of particular interest, are

$$a_1 = \frac{3k_3}{4} e_1^2 e_2 \sin (\omega_c - \omega_m)t \quad (9)$$

and

$$a_2 = \frac{3k_3}{4} e_1 e_2^2 \sin (\omega_c - 2\omega_m)t. \quad (10)$$

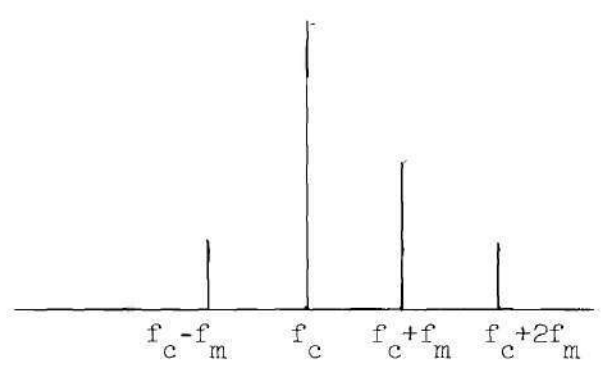
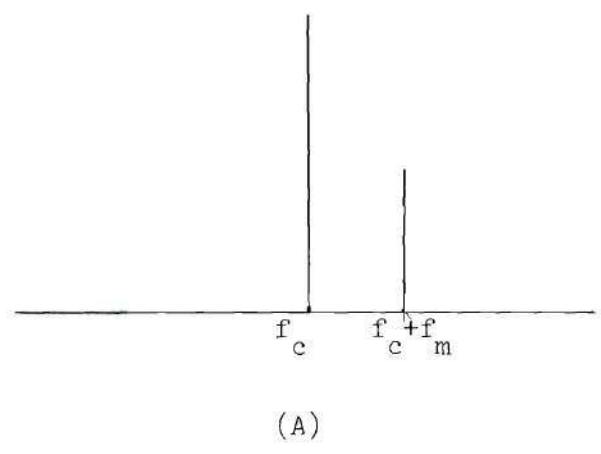


Figure 4. Frequency Spectrum of Single-Sideband Signal Without Intermodulation (A) and With Intermodulation (B).

These terms are known as third-order intermodulation products. Examination of these two terms reveals that they can be made quite small by reducing the carrier amplitude  $e_1$ . In particular, if the carrier amplitude is reduced 40 db,  $a_1$  is reduced 80 db and  $a_2$  40 db. Thus where intermodulation may be occurring within the spectrum analyzer, considerably improvement will be gained by attenuating the carrier. The advantages of reducing the carrier amplitude for the single-sideband case are discussed in detail by Firestone.<sup>3</sup> An illustrative spectrum of  $e_o$  is given by Figure 4(B). It should be noted that intermodulation occurring in the transmitter is indistinguishable from that occurring in the spectrum analyzer, unless certain checks are made. Therefore, if the transmitter is modulated the allowable signal levels applied to the terminals of the spectrum analyzer are quite critical.

The test for spectrum analyzer intermodulation involves the insertion of a known amount of attenuation between the transmitter and spectrum analyzer after the intermodulation product levels are noted. If the intermodulation is in fact occurring within the transmitter, all products being displayed will be attenuated by a greater amount. This is explained by the fact that the amplitudes of the intermodulation products involve a second-order term.

Because the nonlinear effects discussed above, the dynamic range of many spectrum analyzers is limited to 60 db; some types have a dynamic range of even less. Since both government and commercial standards require all spurious outputs of transmitters other than carrier harmonics to be suppressed 80 db, the average spectrum analyzer is unsuitable for

carrier noise and out-of-channel sideband measurements, without the use of suitable devices to attenuate the carrier a minimum of 20 db. Several means of attenuating the carrier can be considered. Some of the possible choices will be discussed in the next section. The purpose of this thesis is to present the results of an investigation of a carrier cancellation scheme to effect the carrier reduction.

## CHAPTER III

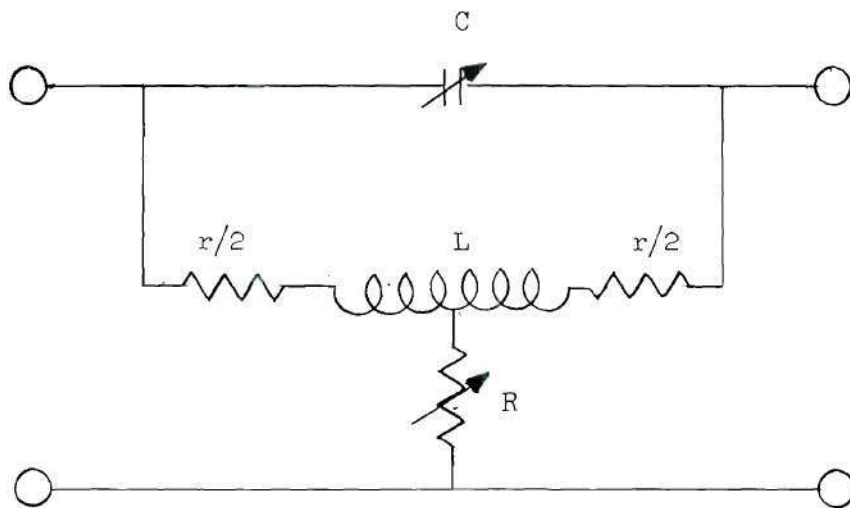
## CARRIER REDUCTION TECHNIQUES

Passive Filter Networks.--Guttwein<sup>4</sup> investigated the use of crystal filters for accomplishing carrier attenuation. He concluded, however, that it would be necessary to cascade several sections to obtain the required band rejection characteristics. A filter of this type would be usable at only one frequency, and in addition crystals have spurious oscillation modes which may occur in the region of measurement interest.

Little discussion of the use of mechanical filters, for the isolation of low level carrier noise and sidebands, appears in the literature; however, the disadvantages of mechanical filters are similar to those of crystal filters, particularly cost and fixed frequency operation.

The bridged-T network has been developed for RF measurements.<sup>5</sup> Figure 5 shows a typical circuit that resulted in a value of  $Q$  of 284. A bridged-T filter was designed for use at Georgia Tech Engineering Experiment Station on Project A-343. The results of this study are presented in the Appendix. The work was quite successful in that a  $Q$  of 425 was obtained using extreme care in construction and tuning. The bridged-T network is apparently quite useful for measurement of carrier or oscillator frequency harmonics.

Active Filter Networks.--The methods discussed in the previous section involved the use of various types of passive band-rejection filter net-



$$\omega^2 = LC$$

$$R = \frac{\omega^2 L^2}{4r}$$

Figure 5. Schematic Diagram of Typical Bridged-T Network

works. Another approach that was not disclosed in the literature would be to selectively amplify the component of the frequency spectrum that is under observation, and combine this component with the original spectrum in such a manner that cancellation of the carrier component will result.

The system that was investigated in this thesis is shown in block diagram form in Figure 6. The signal to be observed is separately passed through two paths, one of which consists of three extremely narrow-band unity-gain amplifiers. The second path passes the signal through a tapped delay line in order to obtain an adjustment of the time relationship of the carrier component voltage. The output of each path is then applied to the control grids of a dual-triode cathode-coupled cathode follower. Since three amplifiers were incorporated, the phase of the carrier component that passed through the upper path in Figure 6 is altered by 180 degrees. Thus, with the proper adjustment of the tapped delay line a phase differential of 180 degrees between the two carrier components is obtained and cancellation is effected in the cathode follower.

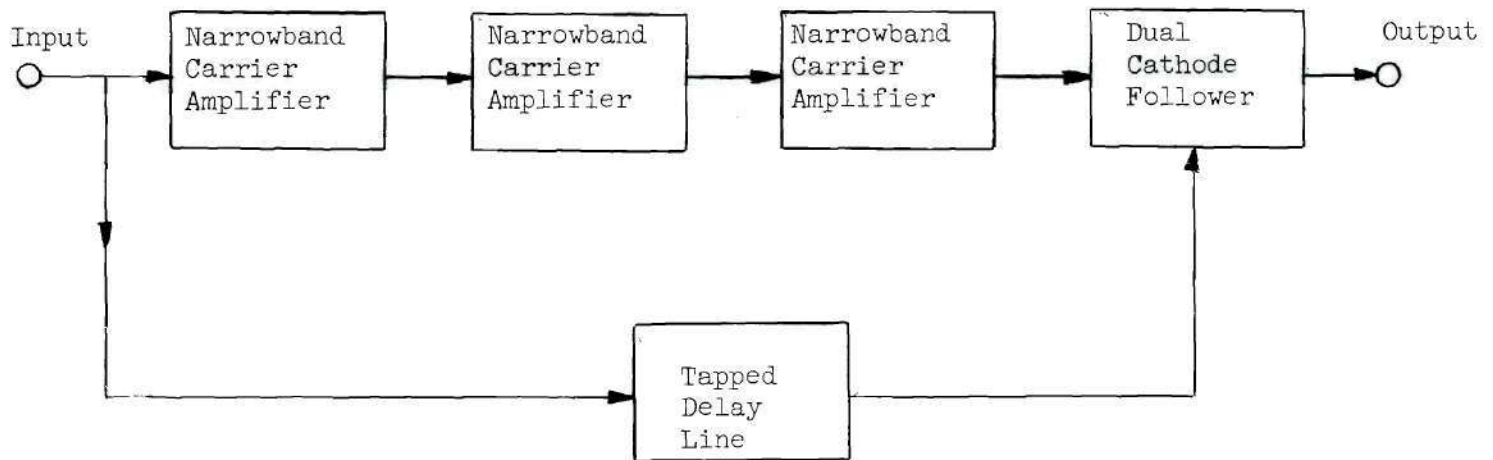


Figure 6. Block Diagram of Carrier-Cancellation Device.

## CHAPTER IV

## DESIGN REQUIREMENTS FOR CARRIER CANCELLATION DEVICE

Introduction.--The design of the device was carried out in four steps. First, the basic design for one amplifier stage was accomplished and then, using the derived circuitry, two additional stages were cascaded with the first. A total of three stages was used in order to accomplish the necessary phase shift of 180 degrees. The circuit for combination of the filtered output of the amplifiers with the original signal was then developed. Finally, a tapped delay line was designed in order to delay the original signal an amount necessary to provide exactly 180 degrees phase differential in the two signals and thereby effect cancellation of the carrier.

The design requirements of the device are as follows:

1. The carrier component of the signal being measured should be attenuated by at least 20 decibels making possible an effective dynamic range of the spectrum analyzer of 80 db.
2. Noise components more than 10 kilocycles from the carrier should not be materially affected.
3. Stability of the carrier attenuation should be such that successive repetitions of the spectrum analyzer sweep give essentially the same carrier amplitudes.
4. The device should be independent of the characteristics of the transmitter under test.

In addition, the cost of the device should be less than mechanical or crystal filters having equivalent transfer characteristics, and the device should be capable of being suitably packaged as an addition to present laboratory equipment.

The design of each component used to achieve these requirements will now be discussed.

Amplifiers.--The primary purpose of the amplifier stages is to provide a narrow bandpass filter so that the carrier component of the input test signal will be passed, while the sidebands will be attenuated. In order to accomplish the desired bandpass characteristics a parallel-resonant inductance capacitance tank circuit is used to provide the plate load impedance for each amplifier stage. Particular emphasis was placed on designing the resonant circuit with a high Q, or center-frequency to half-power bandwidth ratio. Negative feedback was incorporated into each amplifier in order to provide stability against oscillation.

The equivalent circuit for the parallel resonant tank is shown in Figure 7. The effects of insulation losses (leakage) in the condenser C, inductance L, wiring, tube, etc., and the plate resistance  $r_p$  of the tube are represented by R. The series resistance of the coil is represented by r.

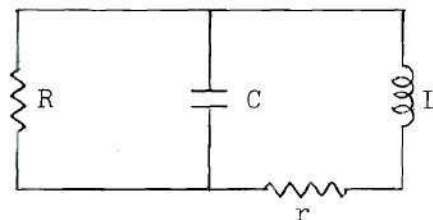


Figure 7. Equivalent Circuit of Plate Load

The selectivity of the circuit of Figure 7 can be derived as follows. Let  $I_1$  represent the current through the capacitor C, and  $I_2$  the current through inductance L and series resistance r; then

$$I_1 = - \frac{E}{\frac{1}{j\omega C}} = - j \omega CE, \quad (11)$$

and 
$$I_2 = \frac{E}{r+j\omega L} = \frac{E}{\sqrt{r^2 + \omega^2 L^2}} \quad \angle - \tan^{-1} \frac{\omega L}{r} ; \quad (12)$$

The quadrature components of the current  $I_2$  can be represented by  $I_r$  and  $I_L$  where

$$I_r = \frac{I_2 r}{\sqrt{r^2 + \omega^2 L^2}} = \frac{r E}{r^2 + \omega^2 L^2} \quad (13)$$

and

$$I_L = \frac{I_2 j\omega L}{\sqrt{r^2 + \omega^2 L^2}} = \frac{j E \omega L}{r^2 + \omega^2 L^2} \quad (14)$$

The r.m.s. value of the total current I is now found to be

$$I = \sqrt{\text{Im}(I)^2 + \text{Re}(I)^2}$$

while reduces to

$$I = E \sqrt{\left( \omega C - \frac{\omega L}{r^2 + \omega^2 L^2} \right)^2 + \left( \frac{r}{r^2 + \omega^2 L^2} \right)^2} \quad (15)$$

Resonance can be defined to be that value of  $\omega$  at which the total current I is in phase with the applied voltage E, i.e., the imaginary

components of the impedance cancel; this will occur when the term

$\left( \omega C - \frac{\omega L}{r^2 + \omega^2 L^2} \right)^2$  reduces to zero, or when the equation

$$\omega C = \frac{\omega L}{r^2 + \omega^2 L^2} \quad (16)$$

is satisfied. Now solving for  $\omega$ ,

$$r^2 + \omega^2 L^2 = \frac{L}{C} \quad (17)$$

$$\omega^2 = \frac{\frac{L}{C} - r^2}{L^2} = \frac{1}{LC} - \frac{r^2}{L^2} \approx \frac{1}{LC} \quad (18)$$

for large values of  $Q$ , where  $Q = \frac{\omega L}{r}$ . From equation (12) the value of the current at resonance is,

$$I = E \left( \frac{r}{r^2 + \omega^2 L^2} \right)^2 = E \frac{r}{r^2 + \omega^2 L^2}$$

If  $r \ll \omega^2 L^2$ , then

$$I \approx \frac{E r}{\omega^2 L^2} \approx E \frac{CR}{L} \approx E \omega_o^2 C^2 r \approx \frac{E}{\omega_o L} \cdot \frac{1}{Q} \approx \frac{\omega_o CE}{Q}, \quad (19)$$

where  $Q = \omega_o L/r$ , and  $I_2 \approx -I_1 \approx E/\omega_o L \approx -\omega_o CE$ . (20)

Now let the equivalent parallel resistance of the series resistance  $r$  be represented by  $R_e$  as shown in Figure 8. Then,

$$R_e = \frac{L}{CR} = Q_e \omega_o L = Q_e / \omega_o C = Q_e \sqrt{L/C} \quad (21)$$

where  $Q_l$  represents the Q of the inductance L, or

$$Q_l = R_e \sqrt{C/L}, \tag{22}$$

Now let R represent the effect of all insulation losses in condenser, coil, wiring, switches and tubes, together with the plate resistance  $r_p$  of the vacuum tube; the resulting circuit is shown in Figure 8. Also, let the resulting parallel resistance be represented by  $R_D$ ; this is the resonant impedance. Thus,

$$R_D = R \parallel R_e = \frac{1}{1/R + Cr/L} \tag{23}$$

The overall Q of the circuit of Figure 8 can now be found by equation (21),

$$Q = \sqrt{\frac{C}{L}} \cdot R_D = \sqrt{\frac{C}{L}} \cdot \frac{1}{1/R + CR/L} = \frac{1}{(1/R) \sqrt{L/C} + r \sqrt{C/L}} = \frac{1}{(\omega_o L/R) + r/\omega_o L} \tag{24}$$

$$Z = R_D \parallel L \parallel C = \frac{1}{1/R_D + \frac{1}{jL} - j\omega C}, \text{ or } |Z| = \frac{1}{\sqrt{\left(\frac{1}{R_D}\right)^2 + (\omega C - 1/\omega L)^2}} = \frac{R_D}{\sqrt{1 + R_D^2 \left(\omega C - \frac{1}{\omega L}\right)^2}} \tag{25}$$

Since  $R_D = Q \omega_o L$ ,  $\omega_o C = \frac{Q}{R_D}$ , and  $\frac{1}{\omega_o L} = \frac{Q}{R_D}$ , then

$$C = \frac{Q}{\omega_o R_D} \text{ and } \frac{1}{L} = \frac{Q \omega_o}{R_D} .$$

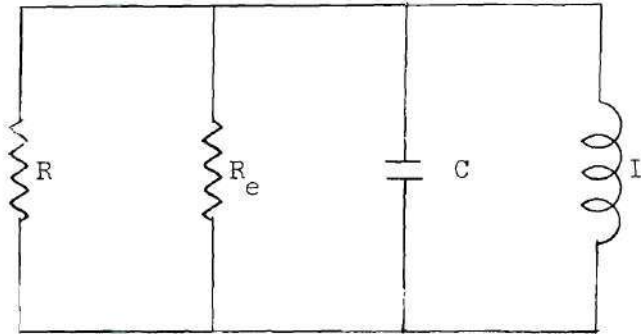


Figure 8. Reduction of Equivalent Circuit.

Thus, the magnitude of the impedance  $Z$  can be given by

$$\begin{aligned}
 |Z| &= \frac{R_D}{\sqrt{1 + R_D^2 \left( \frac{Q \omega}{\omega_o R_D} - \frac{Q \omega_o}{R_D} \right)^2}} \\
 &= \frac{R_D}{\sqrt{1 + Q^2 \left( \frac{\omega}{\omega_o} - \frac{\omega_o}{\omega} \right)^2}}
 \end{aligned} \tag{26}$$

At frequencies other than the resonant frequency, the frequency response of the circuit, or "selectivity", is determined by the ratio of the resonant impedance  $R_D$  to the impedance  $|Z|$  as defined in Equation (26), or

$$\frac{A_o}{A} = \frac{R_D}{|Z|} = \sqrt{1 + Q^2 \left( \frac{f}{f_o} - \frac{f_o}{f} \right)^2} \tag{27}$$

A computer program for determining the overall attenuation response using this equation for three cascaded amplifiers is presented in Appendix

1. The three input parameters are as follows:

$F_0$  = center frequency

$Q$  =  $\frac{\text{center frequency divided by the}}{\text{bandwidth between 3 db points on input response function}}$

$N$  = Number of identical cascaded stages.

The program calculated the attenuation relative to that at the tuned frequency (0 db) for frequencies in increments of 0.1 per cent of the center frequency, until an attenuation of 40 db was reached on each side of the center frequency.

The computer program was used to determine the necessary overall  $Q$  in order to obtain a 10 db bandwidth of 20 kilocycles. Several values of  $Q$  were specified and the corresponding selectivity curves calculated, until the proper curve was obtained. As seen from the data given in Appendix 1, a value of  $Q$  equal to approximately 225 per stage is necessary to accomplish the required selectivity.

Several methods of winding inductances were considered. The use of ferrite cores appeared to offer the highest  $Q$ , and in addition allows the inductances to be made quite small physically. Because of frequency restrictions in the use of ferrite materials, the design frequency of the carrier cancellation device was initially placed at five megacycles.

In order to calculate the required inductance for the circuit of Figure 8, the value of capacitance to be used in the resonant circuit was chosen to be 20 micromicrofarads. This value was selected to approximate the combined effects of the tube capacitance, wiring

capacitance, distributed capacitance of the inductance, and a reasonably small variable capacitor C for tuning the circuit.

The value of the inductance L is now calculated from equation (18), using the value of C of 20  $\mu\mu\text{f}$ ,

$$L = \frac{1}{(\omega_o)^2 C} = \frac{1}{(2\pi \times 5 \times 10^6)^2 (20 \times 10^{-12})}$$

$$= 50 \mu\text{h.}$$

A toroidal ferrite core was commercially available having the following characteristics:

initial permeability,  $\mu_o = 125$  at 1 Mc/s;

loss factor,  $\frac{1}{\mu_o Q} = 0.00002$  at 1 Mc/s,  
 $= 0.00016$  at 10 Mc/s.

For such a core the Q can be calculated to obtain

$$Q = \frac{1}{(0.00002)(125)} = 400 \text{ at 1 Mc/sec,}$$

and

$$Q = \frac{1}{(0.00016)(125)} = 50 \text{ at 10 Mc/sec.}$$

Assuming Q to be inversely proportional to frequency in the range from 1 Mc to 10 Mc, the Q at 5 Mc is found to be approximately  $\frac{400 \times 5}{10} = 200$ .

The required number of turns for each coil can now be found

using the formula<sup>6</sup> for calculating the inductance of toroids wound on ferrite cores,

$$L = (0.0046 N^2 h \log_{10} \frac{OD}{ID}) \text{ in } \mu\text{h} \quad (28)$$

where

$\mu$  = Permeability of material

N = number of turns

h, O.D., I.D. are the dimensions of the ferrite core in centimeters.

From page 25,  $L = 50 \mu\text{h}$  and  $\mu = \mu_0 = 125$ .

The dimensions of the core are as follows:

$$h = 0.42 \text{ cm}$$

$$\text{I.D.} = 1.37 \text{ cm}$$

$$\text{O.D.} = 2.21 \text{ cm}$$

Therefore,

$$\begin{aligned} N^2 &= \frac{L}{0.0046 h \log_{10} \frac{OD}{ID}} \\ &= \frac{50}{(0.0046) (125) (0.42) \log_{10} \frac{2.21}{1.37}} = 1000 \quad (29) \end{aligned}$$

$$N = 31 \text{ turns}$$

In order to verify the previous estimate of Q for ferrite-core toroids, the values of Q for five samples were measured using the test setup shown in Figure 9. Since the isolation between the signal generator

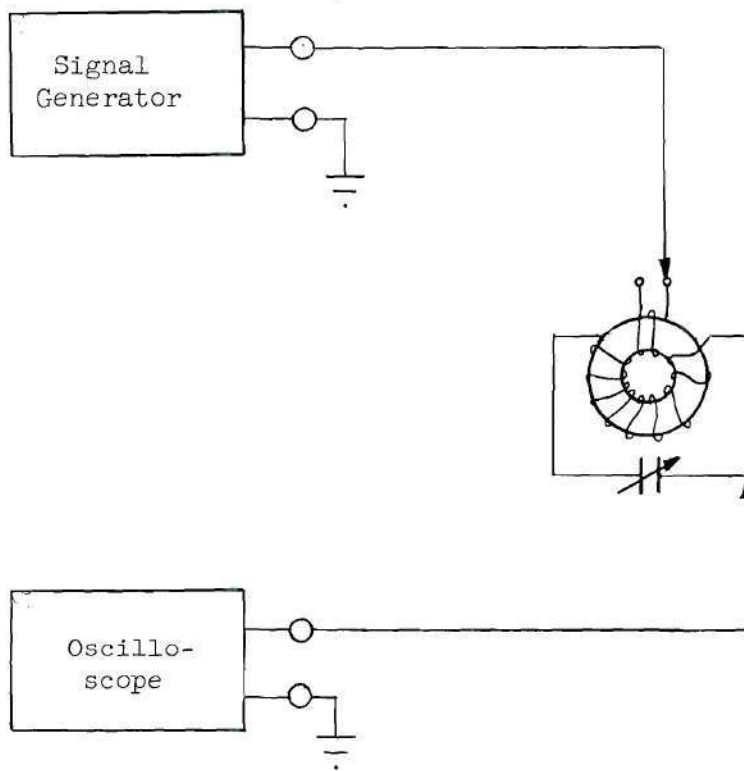


Figure 9. Test Setup for Measuring Q of Toroidal Inductors

output and oscilloscope probe was rather poor, each measurement was discontinued at the point of 10 db attenuation. Due to the absence of any loading effects in this particular test setup, it is believed that the measurements are reasonably accurate to the 10 db points. The results of this test are shown in graphical form in Figure 10.

After determining the characteristics of the five samples at a particular frequency, the relationship between  $Q$  and tuned frequency was determined for one sample. The test setup remained as shown in Figure 9 and the tuned frequency of the tank was changed by varying the value of the capacitor. Figure 11 shows the results of this test.

From these tests it was concluded that the estimate of 200 for the obtainable  $Q$  was somewhat high. This indicates that the  $Q$  does not fall in a linear manner as the operating frequency is increased.

The design of the amplifier is straightforward. A 6AU6 pentode tube was chosen because of the additional plate circuit-to-grid circuit isolation; this reduced any tendency for the amplifier to oscillate. In addition, cathode feedback was used as further insurance against oscillation. The high plate resistance of a pentode makes possible a high  $Q$  due to reduced loading of the tank. A link wound on the tank coil form was used for obtaining the amplifier output. The primary inductance was reduced slightly from that previously calculated to allow a larger variable capacitor to be used for a wider frequency range of operation. The voltage loss from primary to secondary of the tuned circuit, can be calculated as follows:

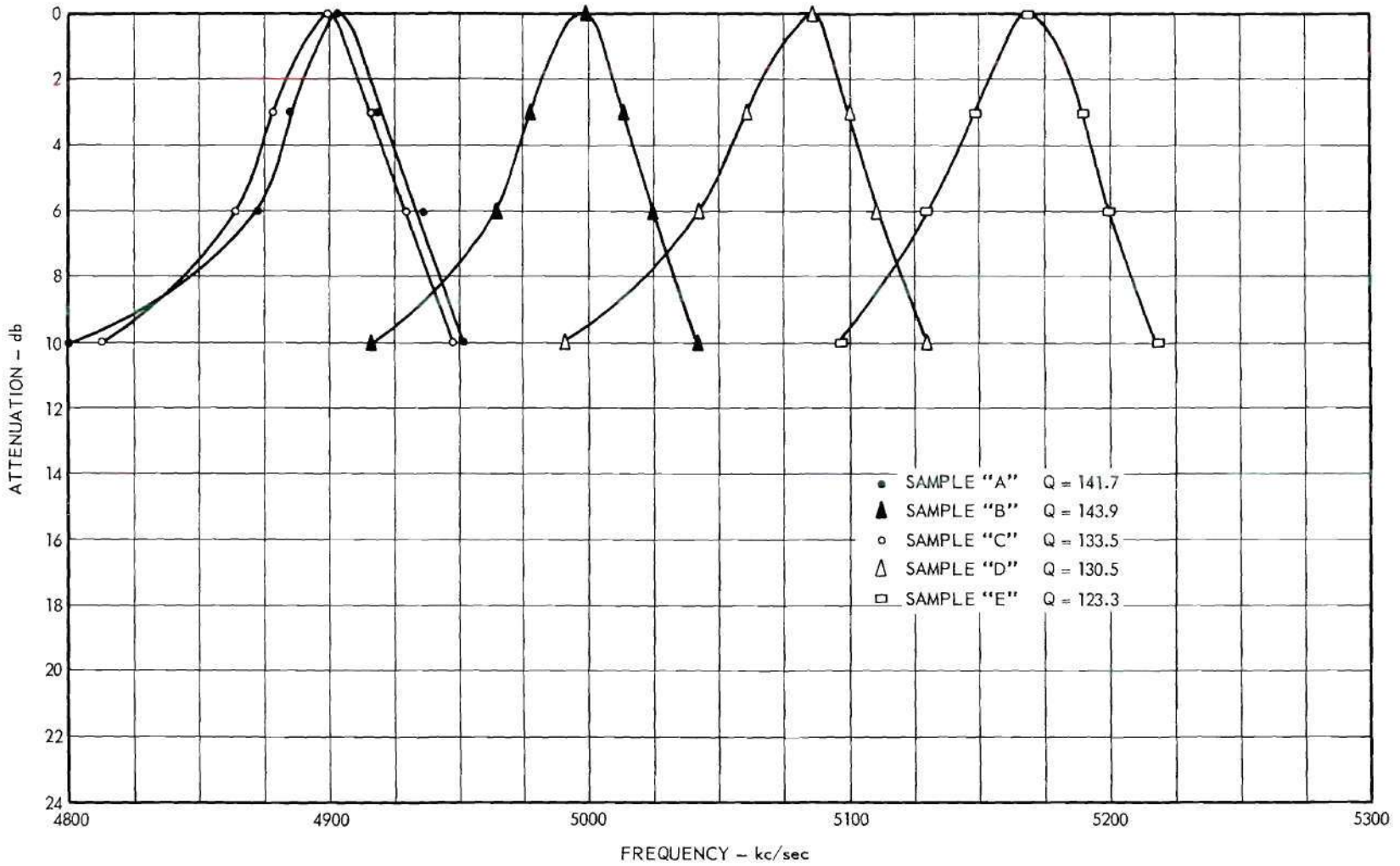


Figure 10. Frequency Response of Five Toroidal Inductances.

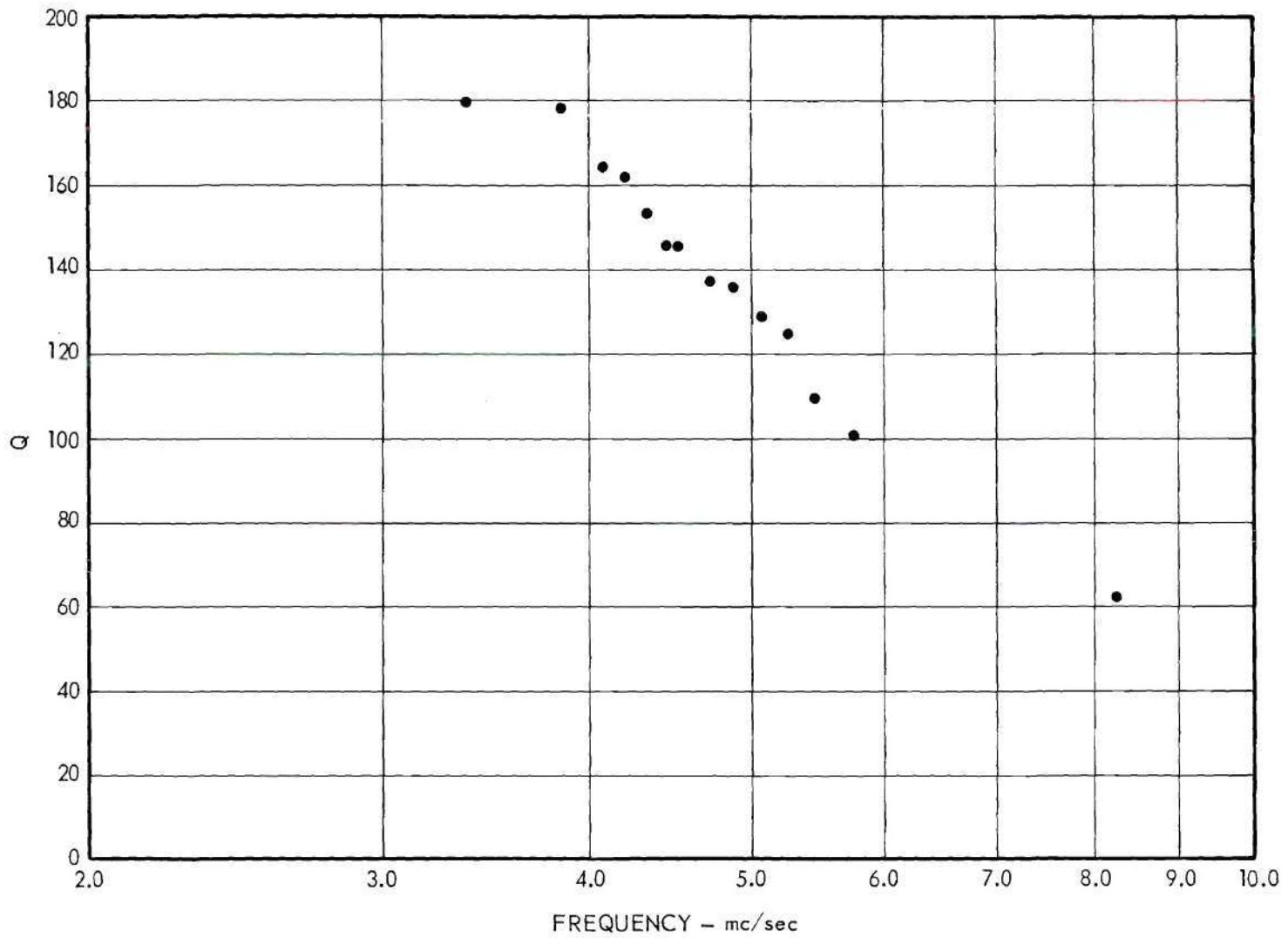


Figure 11. Q Versus Frequency for Toroidal Inductance.

$N_1 = 28 =$  number of turns of primary

$N_2 = 2 =$  number of turns of secondary

$$\frac{E_{\text{pri}}}{E_{\text{sec}}} = \frac{N_1}{N_2} = 14 \text{ (23 db)}$$

To compensate for this loss the amplifier gain should be 23 db. This restriction on gain will be used to determine the proper value of the cathode feedback resistor. The a-c equivalent circuit of one amplifier stage is shown in Figure 12. For this circuit the gain equation is given by<sup>7</sup>

$$A = \frac{g_m R_L}{g_m R_L + (r_p + R_L)/r_p} \quad (30)$$

The parameters for a 6AU6 type pentode are as follows:

$$g_m = 4500 \mu\text{mhos}$$

$$r_p = 1.5 \text{ megohms}$$

The resonant impedance is now found:

$$\begin{aligned} R_L = R_D &= Q \omega_o L = (150) (10\pi \times 10^6) (40 \times 10^{-6}) \\ &= 188,000. \end{aligned}$$

The necessary gain was calculated previously to be 23 db or 14.0. The values of  $R_L$ ,  $g_m$ ,  $r_p$ , and  $A$  may now be substituted into equation (30) to determine  $R_K$ .

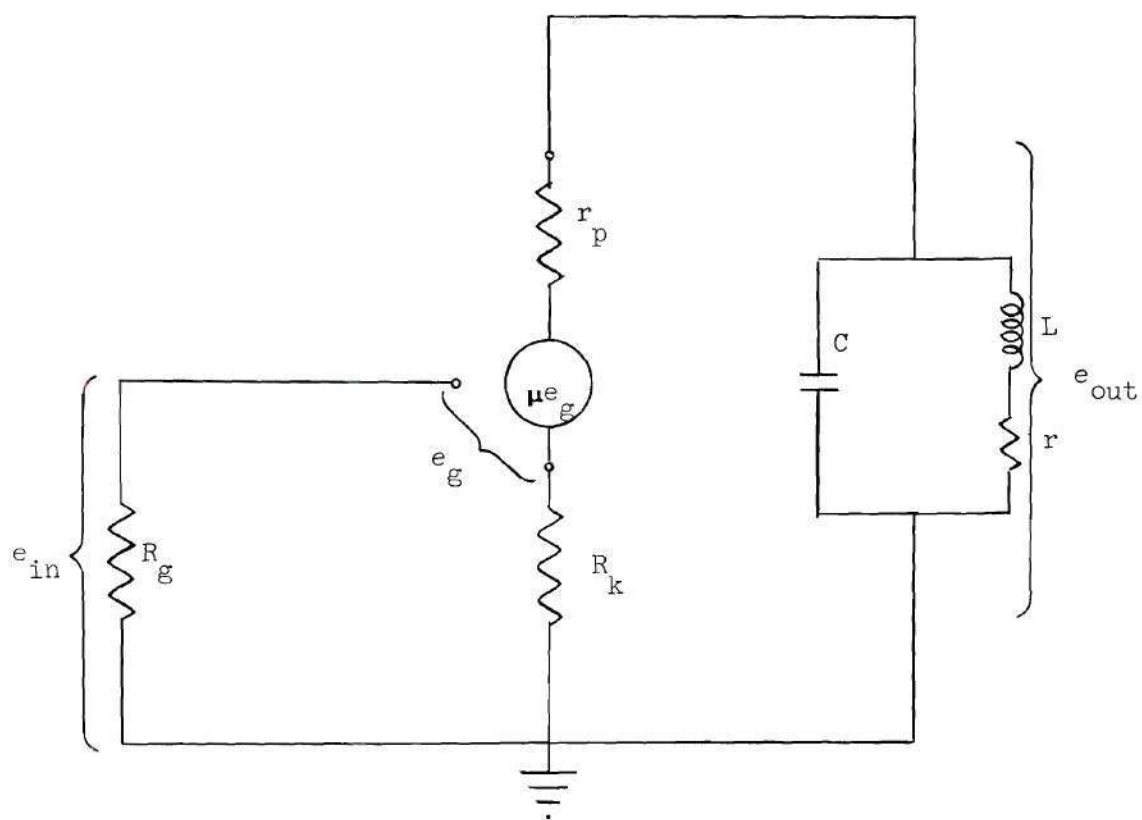


Figure 12. A-c Equivalent Circuit of Amplifier Stage

$$14 = \frac{(4500 \times 10^{-6}) (.188 \times 10^6)}{4500 \times 10^{-6} R_K + (1.5 + .188) \times 10^6 / 1.5 \times 10^6}$$

Therefore,  $R_K = 13000$  ohms.

The value of  $R_K$  was observed to have an effect on the overall  $Q$  of the amplifier; the optimum value of  $R_K$  determined experimentally was 5600 ohms, or slightly less than half the calculated value. The additional gain of 6 db per stage was compensated for through the use of a capacitive divider preceding the first amplifier stage.

The value of  $R_g$  was chosen sufficiently high so that the secondary of the tank circuit of the preceding stage would suffer no decrease in  $Q$  through loading. It was also found experimentally that coaxial cable was not suitable for connecting the coupling link to the grid circuit of the succeeding stage because of capacitive loading of the tank circuit. When coaxial cable was used, the high  $Q$  was destroyed. In addition, it was necessary that the low side of the link be returned to ground through an extremely small capacitor, because of loading.

Bypass capacitor values of 0.005 microfarads were chosen to provide sufficient grounding of any RF voltages on the screen grid and plate voltage supply.

Figure 13 shows the final circuit used for each amplifier stage. Cathode Follower.--The cathode follower was designed to combine the filtered carrier with the original input signal, with an output impedance to match 50 ohms as closely as possible, corresponding to the spectrum analyzer input impedance of 50 ohms.

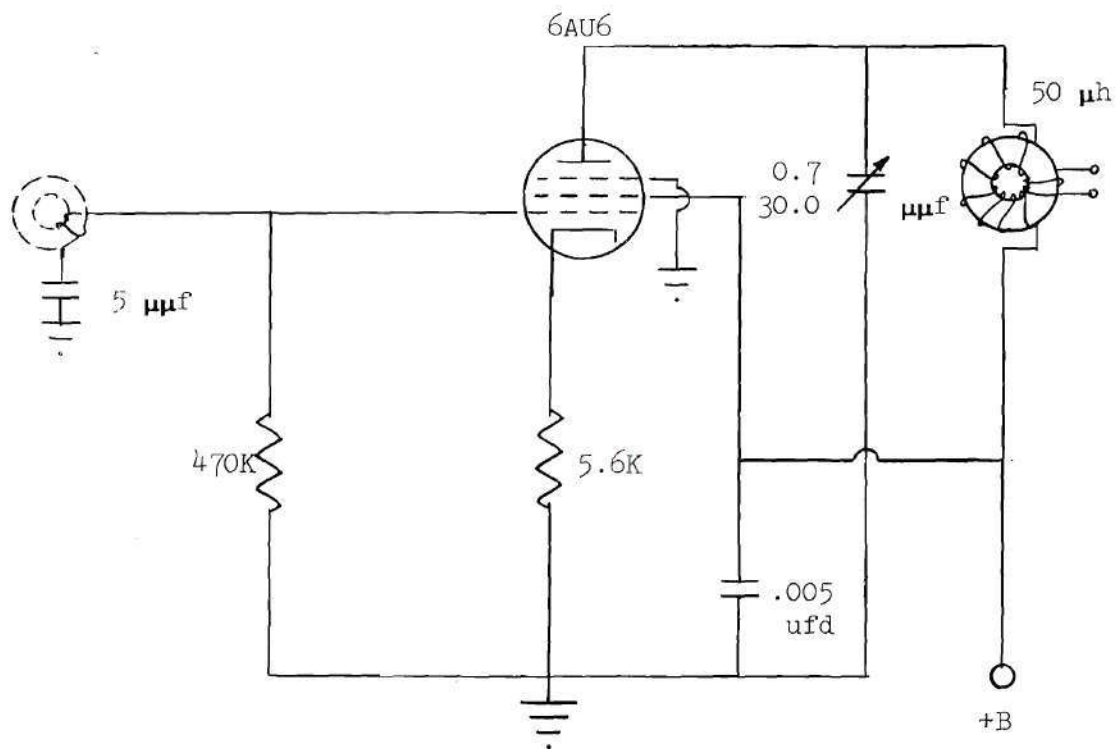


Figure 13. Schematic Diagram of Amplifier Stage.

Since the output impedance of a cathode follower will be approximately  $\frac{1}{g_m}$  a tube was chosen having a value of  $g_m$  as near  $\frac{1}{50}$ , (20,000  $\mu\text{mhos}$ ), as possible

The following data were obtained from a typical tube manual:

Tube Type:	12AT7	12AU7	12AX7
$E_b$	100 250	100 250	100 250 volts
$g_m$	4000 5500	3100 2200	1250 1600 $\mu\text{mhos}$
$r_p$	15000 10900	6500 7700	80000 62500 ohms

The 12AT7 tube was chosen because of the high value of  $g_m$ .

Figure 14 shows the circuit of the cathode follower stage.

From the tube characteristics data,

$$E_b = 250 \text{ V}$$

$$E_c = -2 \text{ V}$$

$$I_b = 10 \text{ ma/section.}$$

Design practice is to set  $R_K$  equal to twice the value of  $r_p$ , or

$$R_K = 2r_p = 2 (10K) = 20 \text{ K,}$$

assuming

$$E_b = 250 \text{ V.}$$

The total resistance in the cathode circuit,  $R_2$ , is now calculated using the desired bias of -2 volts, with total plate current (both triode sections) of 20 ma;

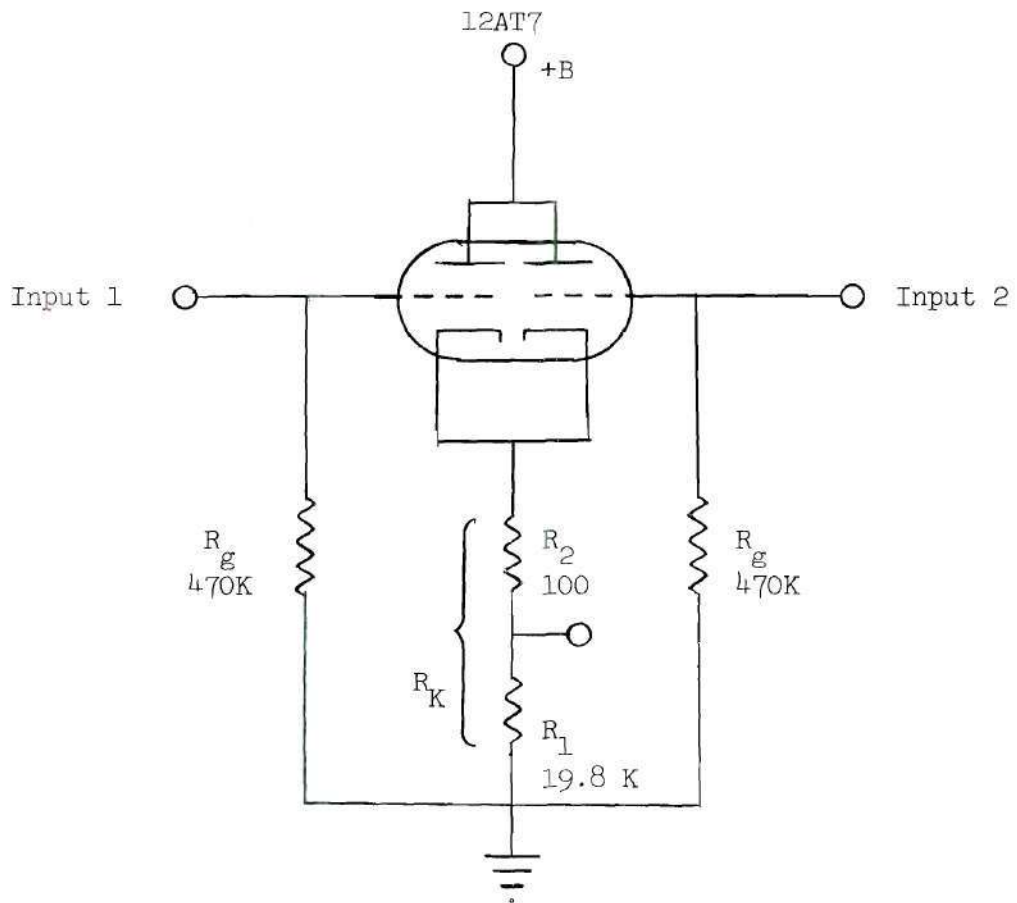


Figure 14. Schematic Diagram of Cathode Follower Circuit.

$$R_2 = \frac{-E_c}{I_b} = \frac{2}{20 \times 10^{-3}} = 100 \text{ ohms.}$$

Therefore,

$$R_1 = R_K - R_2 = 20K - 100 = 19900 \text{ ohms,}$$

if it assumed that  $R_S$  is less than  $0.2 R_g$ , where  $R_s$  is the resistance of the source. The output impedance is determined from the following equation:<sup>8</sup>

$$R_o = \frac{1}{g_m + \frac{1}{R_K} + \frac{2}{r_p}} = \frac{1}{.0005 + .00005 + .0002}$$

$$= 133 \text{ ohms;} \quad (31)$$

As in the amplifier design, a grid resistor value of 470 K was chosen to prevent loading effects in the previous toroidal tank circuit. Delay Line.--A tapped delay line was constructed to provide phase adjustment in order to insure that the two signals arriving at the cathode follower are 180 degrees out of phase.

The circuit in Figure 15 was used. The following equations were used to derive component values.<sup>9</sup>

$$f_c = \frac{1}{\pi \sqrt{LC}}, \quad (32)$$

$$t_s = \frac{1}{\pi f_c} = \sqrt{LC}, \quad (33)$$

and

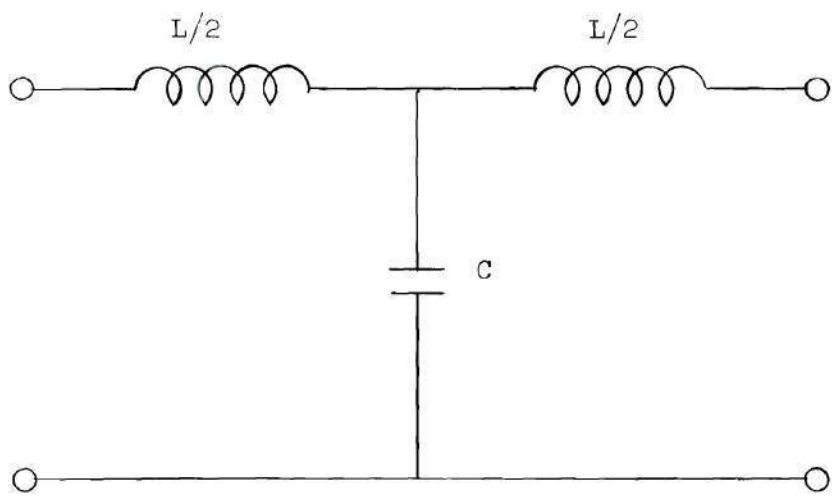


Figure 15. Section of Delay Line.

$$Z_o = \sqrt{\frac{L}{C} [1 - (\frac{f}{f_o})^2]} , \quad (34)$$

where  $f_c$  is the cutoff frequency,  $t_s$  is the time delay per section, and  $Z_o$  is the characteristic impedance. It was assumed that  $Z_o = 50$  ohms,  $f = 0.5 f_c$  and  $f_c = 10$  Mc. Substituting these numbers in equation (32), (33), and (34) yields

$$2500 = \frac{L}{C} (1 - .25),$$

or

$$\frac{L}{C} = 3300;$$

$$f_c = 10^7 = \frac{1}{\pi \sqrt{LC}}$$

$$\pi \sqrt{LC} = 10^{-7}$$

or

$$LC = 10^{-15};$$

since

$$L = 3300 C,$$

then

$$3300C^2 = 10^{-15}$$

$$C^2 = 30 \times 10^{-20};$$

therefore,

$$C = 546 \mu\mu f,$$

$$L = 3300C = 1.8 \mu h,$$

and

$$\begin{aligned}t_s &= \sqrt{LC} = 31.2 \times 10^{-9} \\ &= .032 \mu\text{sec/section.}\end{aligned}$$

Six sections were used to give an adjustment range of approximately one-half cycle.

## CHAPTER V

## EXPERIMENTAL RESULTS

The tests listed below were performed on the device to determine if the device operated satisfactorily and if the design criteria were met.

Frequency Response Characteristics of Single Amplifier Stage.--Two methods were used for measuring the transfer characteristics of the amplifier circuit. For the first method, the test setup shown in Figure 16 was used. A signal generator was applied to the input of one amplifier stage and its output voltage monitored by means of an oscilloscope, while the frequency of the signal generator was varied. The measured data is presented in graphical form in Figure 17.

The second method involved photographing the spectrum analyzer display with the amplifier stage output signal applied. The signal generator was modulated with a noise generator having a flat frequency spectral distribution to 500 kc. The amplifier output spectral distribution therefore approximates the transfer characteristics, since the modulator frequency response in the signal generator is substantially flat. Figure 18 is a photograph of the single amplifier stage output frequency spectrum. The sweep width of the spectrum analyzer was set for 100 kc. The 3-db bandwidth, as measured from the photograph, is approximately 40 kc. For comparison, Figure 19 shows the spectrum of the signal generator with modulation as described above. The correspond-

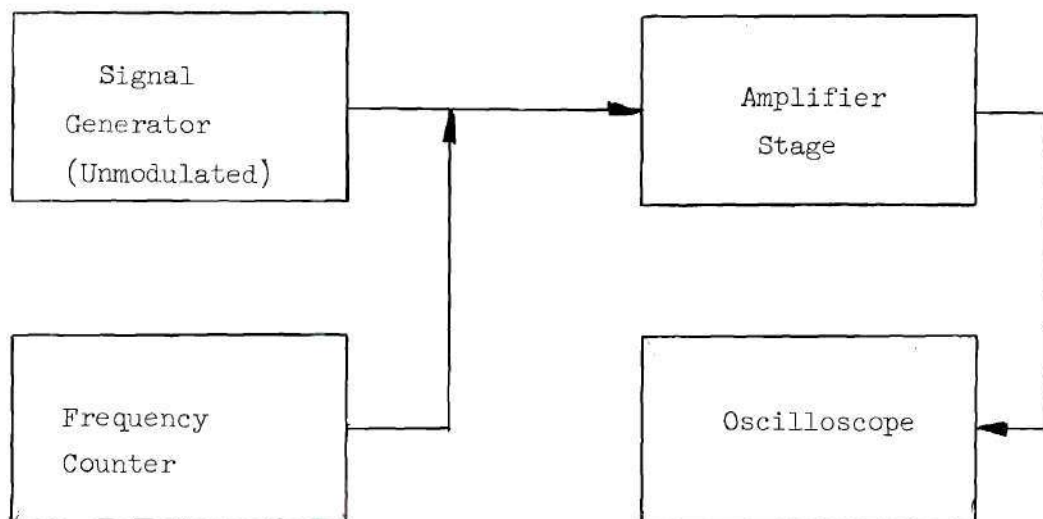


Figure 16. Test Setup for Measuring Frequency Response of Single Amplifier Stage.

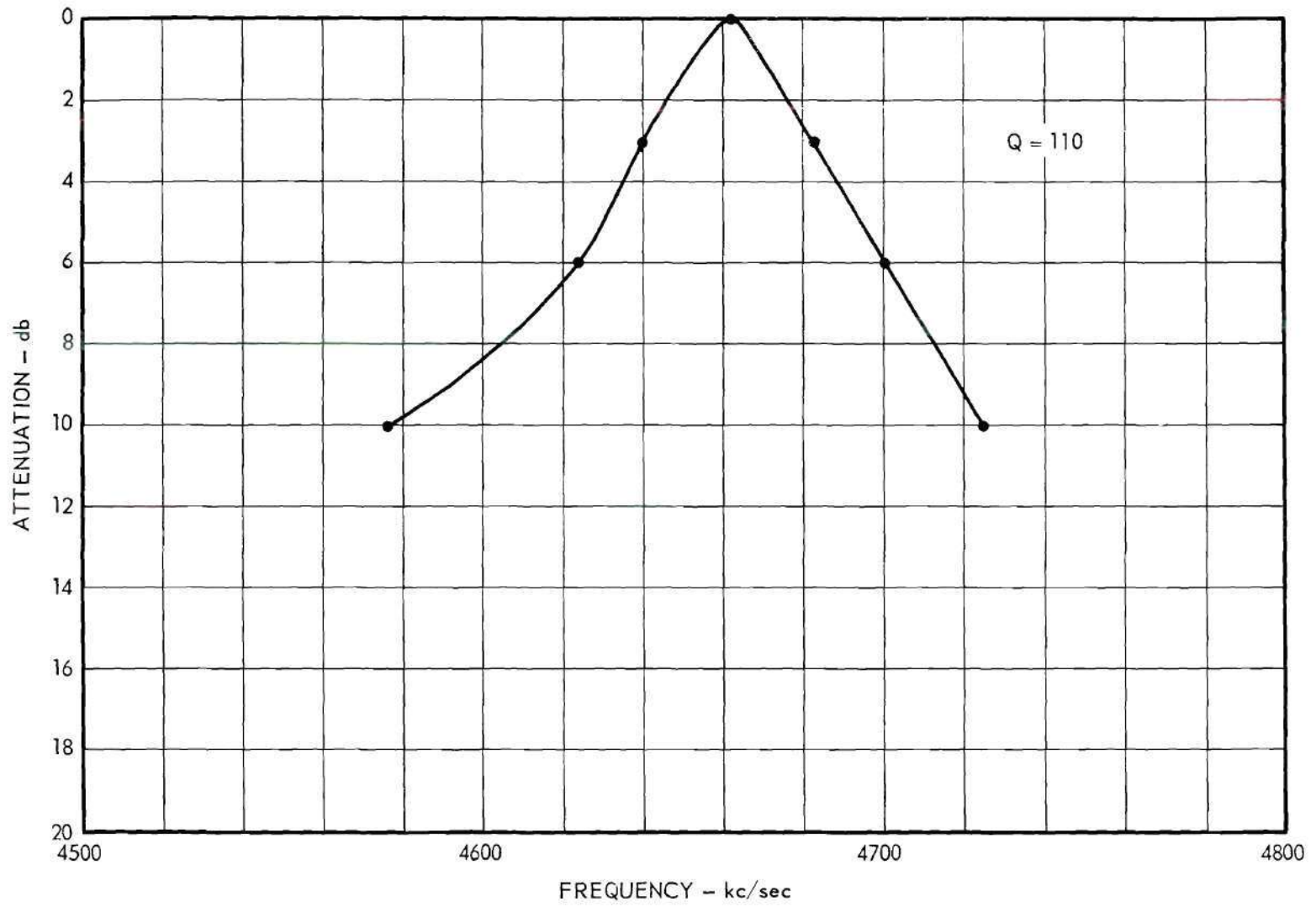


Figure 17. Frequency Response of Single Amplifier Stage.

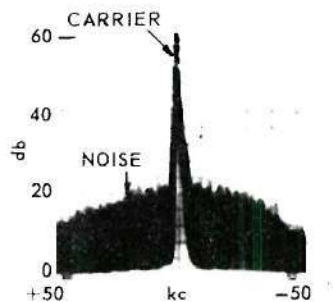


Figure 18. Display of Power Density Spectrum of Output of Single Amplifier Stage. Signal Modulated 10% by 500 Kc Random Noise.

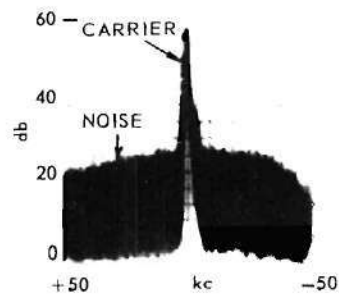


Figure 19. Display of Power Density Spectrum of Input to Amplifier Stage in Figure 17.

ing value of  $Q$  may be calculated as follows:

$$Q = \frac{f_o}{\Delta f} = \frac{4.75}{40} = 118.$$

This value compares closely with that obtained using the first method. Both values are somewhat lower than the values for the five samples given previously. This is a logical result of the loading effects of the tube which tend to broaden the response of the tuned circuit.

Frequency Response of Three Cascaded Amplifiers.--This test was conducted using three methods. The first two methods are identical with the two in the previous test. Figure 20 presents the graphical results of the method in which the frequency of an unmodulated signal was varied and the output voltage recorded. From these data the bandwidth is found to be 3 kc.

The second method involved photographing the noise modulated spectrum as before. The photograph obtained is shown in Figure 21.

The third method involves the use of a sweep generator, as shown in the test setup of Figure 22. The indicated deviation was  $\pm 30$  kc; the half-power bandwidth therefore is approximately 6 kc, as obtained from the photograph in Figure 23. This compares favorably with the results of the first method. It should be pointed out that the  $Q$  can be calculated, using this value of 6 kc, to be approximately 800. This is considerably higher than the expected value of approximately 400, and is very likely an indication of a small amount of positive feedback caused by inductive coupling between components of the amplifiers.

Response of Device with Carrier Cancellation, Tone-Modulated Input Signal.--Several different test methods were used for determining the

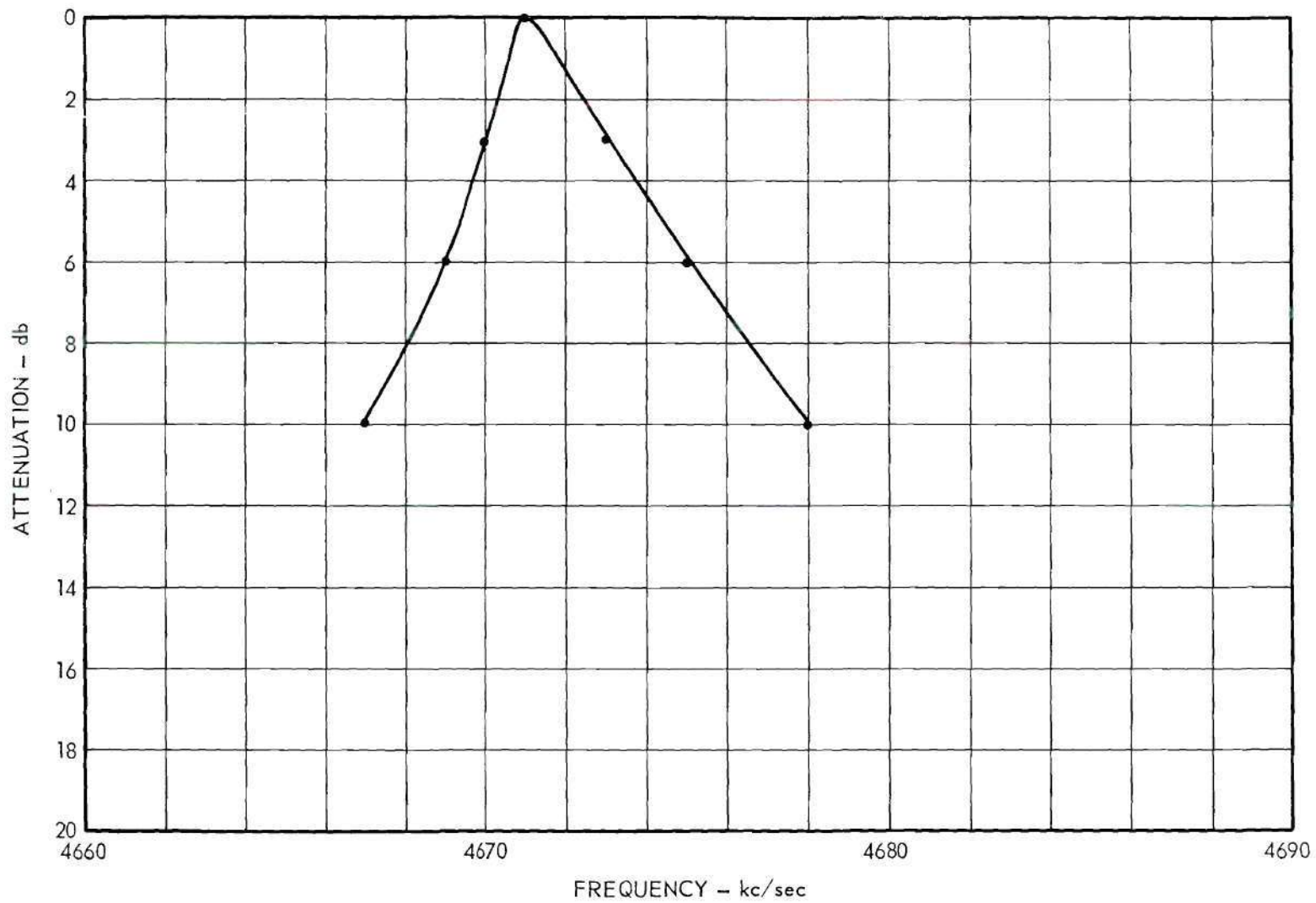


Figure 20. Frequency Response of Three-Stage Amplifier.

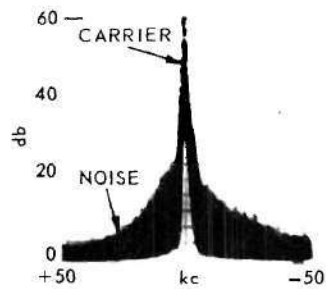


Figure 21. Display of Power Density Spectrum of Output of Three Cascaded Amplifier Stages. Signal Modulated 10% by 500 Kc Random Noise.

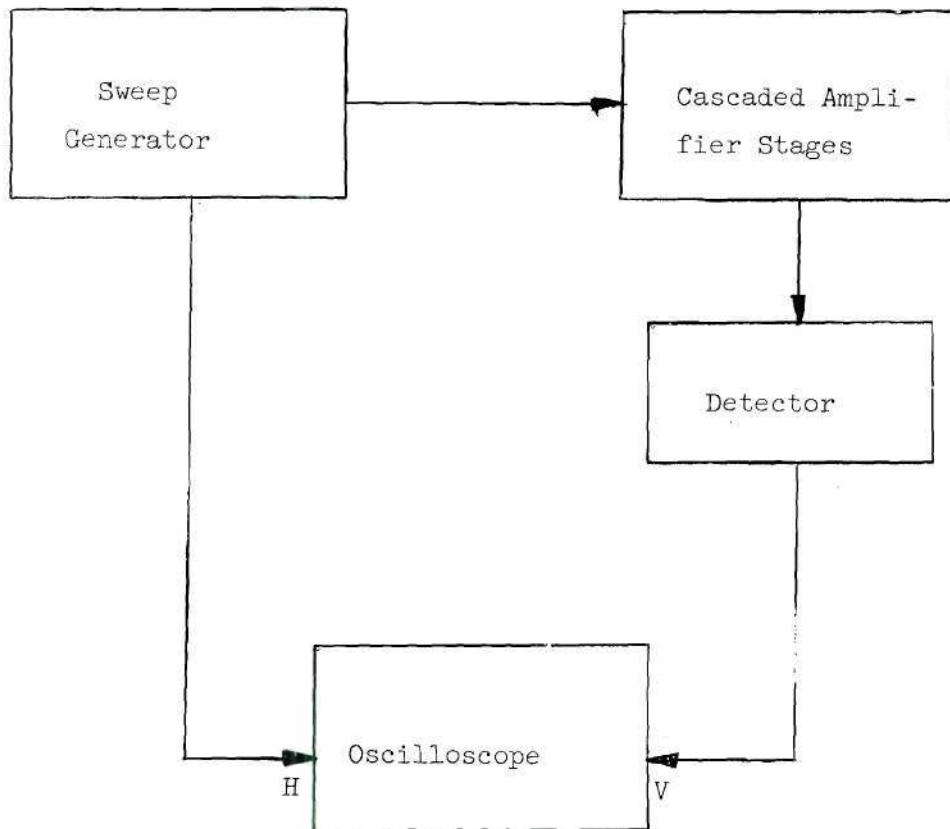


Figure 22. Setup for Measuring Amplifier Bandwidth Using Sweep Generator.

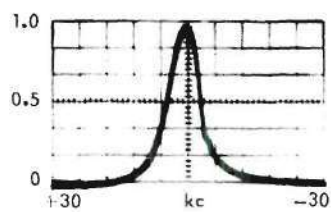


Figure 23. Frequency Characteristics of Three Cascaded Amplifier Stages Using Sweep Generator.

frequency characteristics of the entire network. First, the attenuation at the tuned, or carrier, frequency was determined by applying an unmodulated signal to the device and photographing the spectrum analyzer display, both with and without cancellation. A photograph of the display without cancellation is shown in Figure 24. The carrier signal extends 20 db beyond the scale, or 60 db above the baseline. Figure 25 is a photograph of the spectrum analyzer with cancellation. The carrier has been attenuated to a level of 20 db above the baseline; the carrier attenuation is therefore 40 db. The signal generator was then modulated by a 10 kc audio tone at 10 per cent and the spectrum photographed. Figure 26 shows the spectrum without carrier cancellation, and Figure 27 shows the results with cancellation. The carrier again extended 20 db above the scale in Figure 26. The carrier was again reduced by about 40 db, and the sidebands were reduced approximately 10 db. The modulating frequency was then increased to 15 kc and photographs made, first of the carrier and upper sideband, without cancellation, Figure 29; the carrier and lower sideband were similarly photographed, Figures 30 and 31. The carrier was reduced 40 db, and sidebands 5 to 8 db. In addition to photographing the tone-modulated spectra, the overall response was also obtained using an unmodulated signal and plotting the response of the device at various frequencies about the tuned frequency. The resulting curve is shown in Figure 32, and verifies the sideband attenuation as seen in the photographs.

#### Response of Device with Carrier Cancellation, Noise-Modulated Input

Signal.--To determine the frequency characteristics of the device,

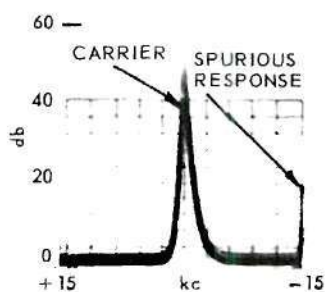


Figure 24. Display of Output Power Density Spectrum of Cancellation Device without Carrier Cancellation. Input Signal Unmodulated.

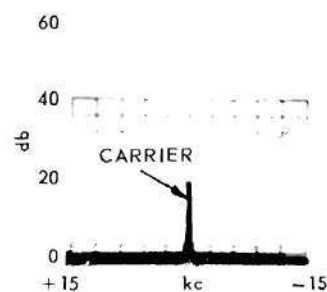


Figure 25. Display of Output Power Density Spectrum of Cancellation Device with 40 db Carrier Cancellation. Input Signal Unmodulated.

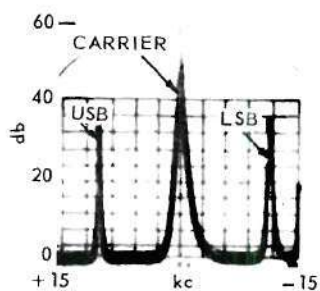


Figure 26. Display of Output Power Density Spectrum of Cancellation Device without Cancellation. Input Signal Modulated 10% by 10 Kc Tone.

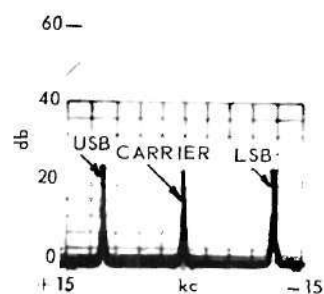


Figure 27. Display of Output Power Density Spectrum of Cancellation Device with 40 db Carrier Cancellation. Input Signal Modulated 10% by 10 Kc Tone.

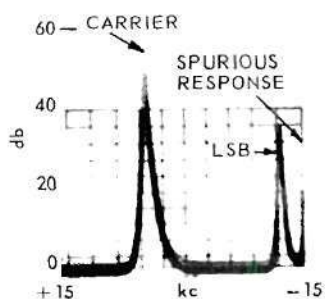


Figure 28. Display of Output Power Density Spectrum of Cancellation Device without Carrier Cancellation. Input Signal Modulated 10% by 15 Kc Tone. Carrier and Lower Sideband.

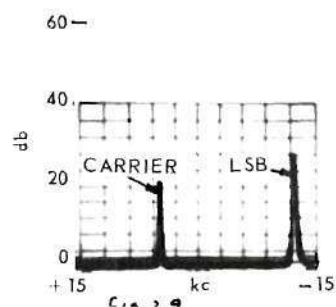


Figure 29. Display of Output Power Density Spectrum of Cancellation Device with 40 db Carrier Cancellation. Input Signal Modulated 10% by 15 Kc Tone. Carrier and Lower Sideband.

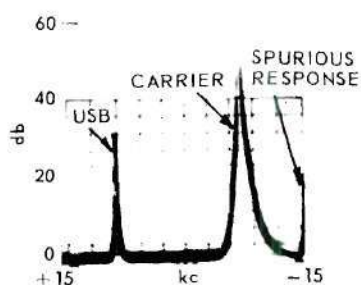


Figure 30. Display of Output Power Density Spectrum of Cancellation Device without Carrier Cancellation. Input Signal Modulated 10% by 15 Kc Tone. Carrier and Upper Sideband.

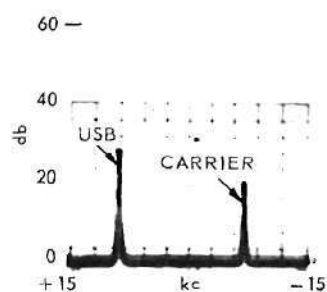


Figure 31. Display of Output Power Density Spectrum of Cancellation Device with 40 db Carrier Cancellation. Input Signal Modulated 10% by 15 Kc Tone. Carrier and Upper Sideband.

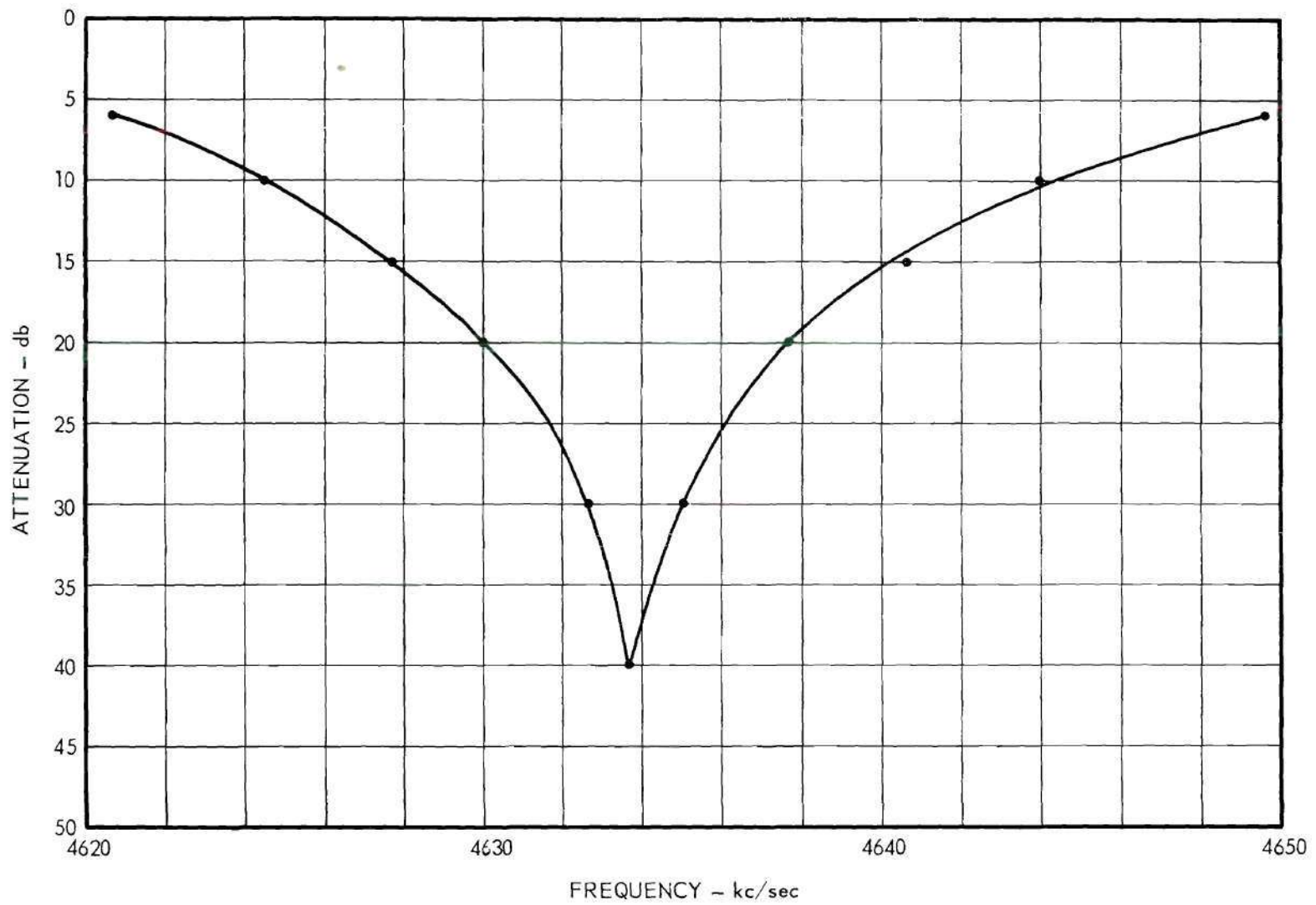


Figure 32. Frequency Response of Overall Circuitry.

the test signal was modulated by noise having a flat spectrum to 500 kc, at 10 per cent. Figure 33 shows the results as displayed by the spectrum analyzer. The sweep width was adjusted to 100 kc. Carrier suppression was 40 db. It can be seen from the photograph that the noise is not appreciably affected at frequency separations greater than 15 kc from the carrier. For comparison Figure 34 shows the spectrum of the test signal when applied directly to the spectrum analyzer. It is important to note that some photographs taken of signals without carrier cancellation have spurious signals appearing at the edge of the displayed spectrum. These are generated within the spectrum analyzer and are caused by the excessive level of the carrier. These results compare favorably with those in the previous test, in which the input signal was tone-modulated.

Noise Level of Device.--The spectrum analyzer display was photographed with no test signal applied to the device. This is shown in Figure 35. The device was then removed from the spectrum analyzer and the display photographed, Figure 36. The gain controls of the spectrum analyzer were adjusted for maximum dynamic range, as before. The noise contributed by the device is seen to be 40 db below a full scale deflection. With carrier suppression of 40 db and spectrum analyzer gain adjusted for full-scale carrier deflection, the noise contribution is more than 80 db below the actual carrier level.

Noise and Distortion of Typical AM Transmitter.--A typical 400-watt HF AM transmitter was examined to determine the suitability of the device for measurement of carrier noise and sideband splatter. The transmitter

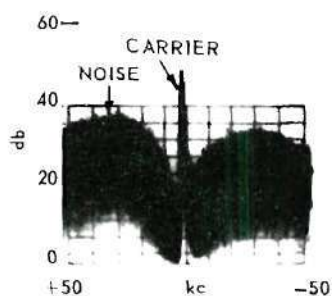


Figure 33. Display of Output Power Density Spectrum of Cancellation Device with 40 db Carrier Cancellation. Input Signal Modulated 10% by 500 Kc Random Noise.

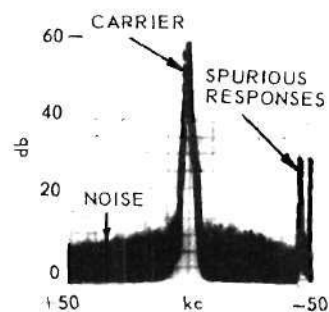


Figure 34. Display of Output Power Density Spectrum of Cancellation Device without Carrier Cancellation. Input Signal Modulated 10% by 500 Kc Random Noise.

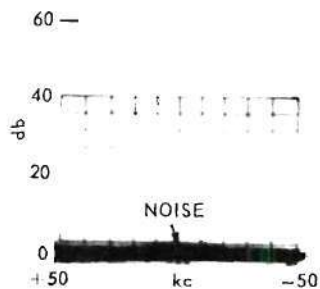


Figure 35. Display of Output Power Density Spectrum of Cancellation Device Showing Residual Noise with no Input Signal.

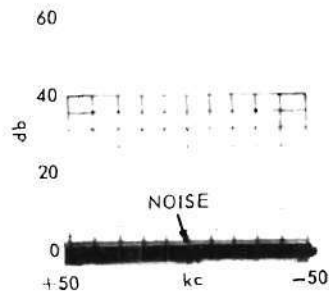


Figure 36. Display of Spectrum Analyzer with no Input to Spectrum Analyzer.

was first modulated with an audio-frequency tone of 3 kc at 100 per cent. Figure 37 shows the spectrum as normally displayed, without carrier cancellation. The base line is 60 db below the carrier and sweep width is 100 kc. It is clear from this photograph that examination of distortion products below a level of -60 db with reference to the carrier is not possible. Figure 38, however, shows the results with the carrier reduced approximately 30 db and the sensitivity of the spectrum analyzer increased 20 db. The range of the instrument has been increased to 80 db. The distortion products are found to extend to the eleventh order, before a level of 80 db below the carrier is reached. The unmodulated transmitter carrier was then examined for noise. Figure 39 shows the spectrum analyzer display with no carrier cancellation. The dynamic range is 60 db. No noise spectral components are visible. With 40 db reduction in carrier amplitude, however, as shown in Figure 40 noise is clearly visible at a level approximately 75 db below the unattenuated carrier. As before, the sensitivity of the spectrum analyzer was increased 20 db. This test proves conclusively that the dynamic range of the spectrum analyzer may be increased to 80 db through the use of the carrier cancellation technique.

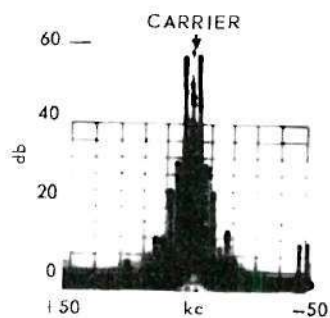


Figure 37. Display of Output Power Density Spectrum of Cancellation Device without Carrier Cancellation. Input Signal from Test Transmitter Modulated 100% by 3 Kc Tone. Visible Distortion Products Extend to 60 db below Carrier.

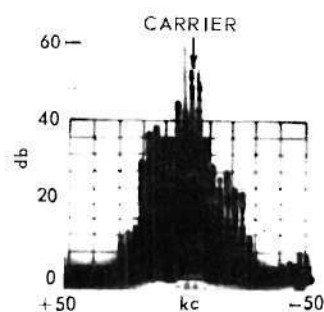


Figure 38. Display of Output Power Density Spectrum of Cancellation Device with 30 db Carrier Cancellation. Input Signal from Test Transmitter Modulated 100% by 3 Kc Tone. Visible Distortion Products Extend to 80 db below Carrier.

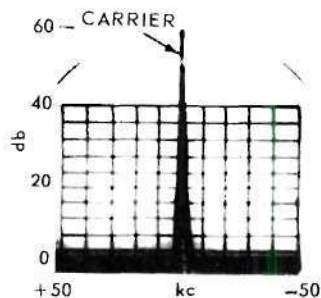


Figure 39. Display of Output Power Density Spectrum of Cancellation Device without Carrier Cancellation. Input Signal from Unmodulated Test Transmitter. Noise Components not Visible.

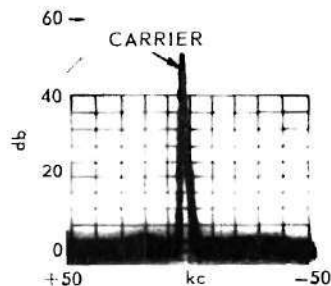


Figure 40. Display of Output Power Density Spectrum of Cancellation Device with 40 db Carrier Cancellation. Input Signal from Unmodulated Test Transmitter. Noise Components Visible 75 db Below Carrier.

## CHAPTER VI

## CONCLUSIONS AND RECOMMENDATIONS

The investigation of this thesis into the use of carrier cancellation for extending the dynamic range of spectrum analyzers resulted in development of a device which successfully reduces the carrier amplitude 40 db, while providing sufficient selectivity to allow measurement of transmitter radiation occurring 20 kilocycles from the carrier with little error. A photograph of the device is shown in Figure 41.

The results of a number of tests described in Chapter V will now be examined and compared with each design criterion to determine the degree of success of the investigation.

The first criterion specified a minimum of 20 db in carrier reduction. The results of the Response of Device with Carrier Cancellation, Tone-Modulated Input Signal test and Response of Device with Carrier Cancellation, Noise-Modulated Input Signal test show that consistent reduction of the 40 db in carrier amplitude is obtainable. With 100 per cent modulation of the test signal, reduction of 30 db was obtained in the Noise and Distortion of Typical AM Transmitter test.

The second criterion stipulated that spectral components of the signal under test that were more than 10 kilocycles removed from the carrier frequency not be significantly affected. The results of the

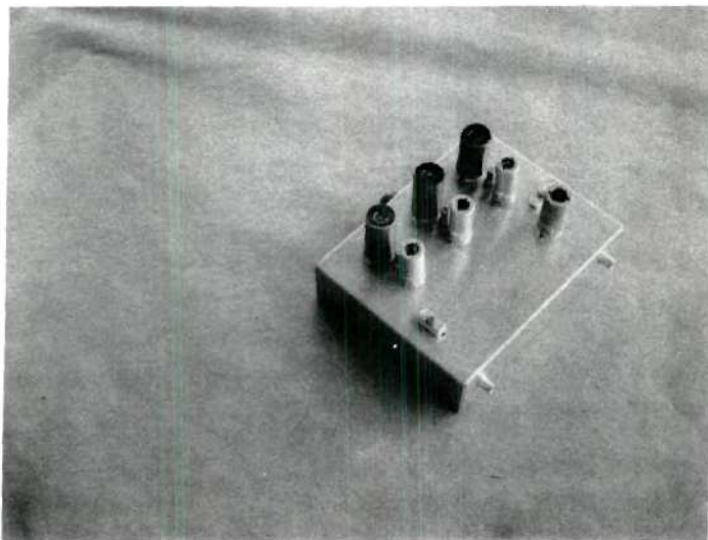


Figure 41 Photograph of Carrier Cancellation Device.

tests above indicate that this was not fully realized. However, spectral components more than 15 kc from the carrier are not adversely affected. The inability to realize this criterion was due to inadequate selectivity of the device, and could be achieved through the use of additional bandpass amplifier stages.

The third criterion stated that the stability of the device should be such that successive repetitions of the spectrum analyzer sweep give essentially the same carrier amplitude. The numerous photographs presented in this thesis which show carrier reduction of 40 db verify the accomplishment of this criterion.

The fourth criterion required the device to be independent of the characteristics of the transmitter under test. The test results of the device using both signal generators and a commercial AM transmitter indicate that the device will operate satisfactorily independently of the type of signal source. Ordinarily, a coupling factor of at least 30 db is required to reduce the test signal to a usable power level. This insures sufficient isolation between the device and signal source.

The carrier cancellation device could be improved considerably through the use of two additional bandpass amplifier stages. The apparent limitation to the number of possible stages is the tendency of a very narrow-band amplifier to oscillate. However, adequate shielding should preclude oscillation with five and possibly seven stages.

Several fields of study exist in which the cancellation device would prove useful. The most important and relatively untouched field

is that of studying exhaustively the frequency characteristics of carrier noise. Another area in which the device could be used is in measuring correlation of carrier noise. If the delay line presently used in the device were extended to provide a delay of several cycles, uncorrelated noise components in the immediate vicinity of the carrier would be found to add, whereas noise components having a sufficient degree of correlation would tend to cancel as does the carrier component. Thus, by observing the spectrum of a signal having noise sidebands, a measure of the correlation might be obtainable.

It is recommended that the device be suitably modified and improved to determine the practical limit in selectivity, and that studies be made of the characteristics of carrier noise through the use of the device.

## APPENDIX A

## COMPUTER PROGRAM FOR CALCULATING SELECTIVITY OF BANDPASS AMPLIFIER

```

INTEGER Q,N                                     $
COMMENCE..READ($$DATA)                         $
WRITE($$FRMT1)                                  $
F=FO                                             $
DF=0.001F                                       $
START..UNTIL A GEQ 40.0                         $
BEGIN CALC..A=LON(0.4343)LOG(SQRT(1+(Q*2)(F/FO-FO/F)*2)) $
WRITE($$RESULTS,FRMT2)                         $
F=F+DF                                          $
END                                              $
IF DF GTR 0                                     $
BEGIN F=FO                                       $
DF=-0.001F                                       $
A=0.0                                           $
GO TO START END                                 $
A=0.0                                           $
GO TO COMMENCE                                  $
INPUT DATA(FO,Q,N)                             $
OUTPUT RESULTS(F,A)                             $
FORMAT FRMT1(W3,B15,*FREQUENCY*,B20,*ATTENUATION*,W0,B18,*MCS*,B28,
*DB*,W4,W4),

```

FRMT2(B17,X6.3,B25,X5.2,W0)

\$

FINISH

\$

COMPILED PROGRAM ENDS AT 0320

PROGRAM VARIABLES BEGIN AT 4415

TABLE 1A

SAMPLE DATA OBTAINED FOR THREE STAGES WITH

Q EQUAL TO 255 PER STAGE

<u>Frequency</u> Mcs	<u>Attenuation</u> Db
4.750	.00
4.754	1.20
4.759	3.85
4.764	6.74
4.769	9.39
4.773	11.71
4.778	13.74
4.783	15.53
4.788	17.12
4.792	18.55
4.797	19.84
4.802	21.03
4.807	22.11
4.811	23.12
4.816	24.05
4.821	24.92
4.826	25.74
4.830	26.51
4.835	27.23
4.840	27.92
4.845	28.58
4.849	29.20
4.854	29.79
4.859	30.36
4.864	30.90
4.868	31.42
4.873	31.92
4.878	32.41
4.883	32.87
4.887	33.32
4.892	33.75
4.897	34.17
4.902	34.58
4.906	34.97
4.911	35.35

TABLE 1A (Continued)

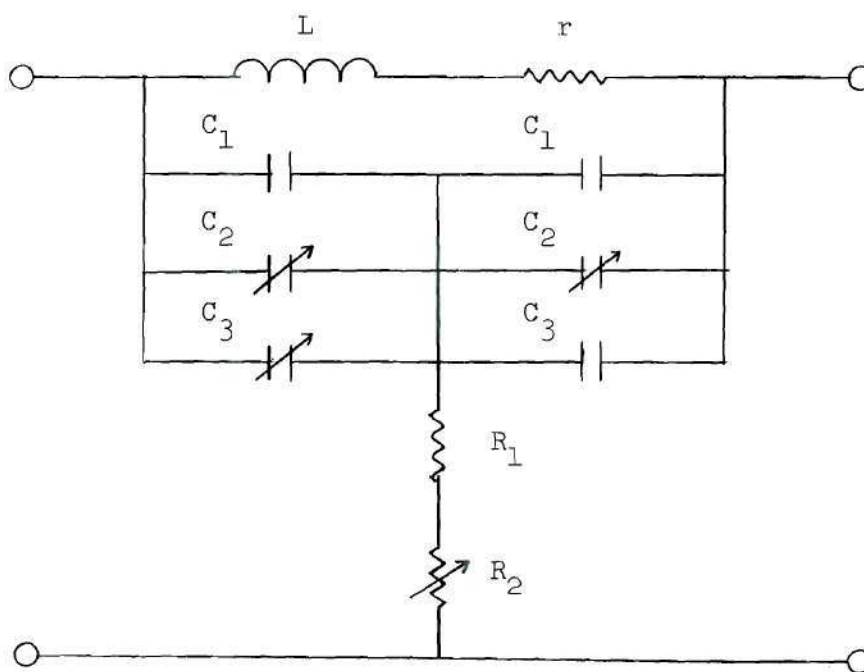
<u>Frequency</u> Mcs	<u>Attenuation</u> Db
4.916	35.72
4.921	36.08
4.925	36.43
4.930	36.77
4.935	37.10
4.940	37.42
4.944	37.74
4.949	38.04
4.954	38.34
4.959	38.64
4.963	38.92
4.968	39.20
4.973	39.47
4.978	39.74
4.982	40.00
4.750	.00
4.745	1.20
4.740	3.87
4.735	6.77
4.731	9.42
4.726	11.76
4.721	13.81
4.716	15.61
4.712	17.22
4.707	18.66
4.702	19.97
4.697	21.16
4.693	22.26
4.688	23.28
4.683	24.23
4.678	25.11
4.674	25.94
4.669	26.73
4.664	27.47
4.659	28.17
4.655	28.83
4.650	29.47
4.645	30.07
4.640	30.66
4.636	31.21
4.631	31.75
4.626	32.26
4.621	32.76

TABLE 1A (Continued)

<u>Frequency</u> Mcs	<u>Attenuation</u> Db
4.617	33.23
4.612	33.69
4.607	34.14
4.602	34.57
4.598	34.99
4.593	35.40
4.588	35.79
4.583	36.17
4.579	36.55
4.574	36.91
4.569	37.26
4.564	37.61
4.560	37.94
4.555	38.27
4.550	38.59
4.545	38.90
4.541	39.21
4.536	39.51
4.531	39.80
4.525	40.09

## APPENDIX B

## BRIDGED "T" FILTER DESIGN



$$f_c = 10 \text{ Mc}$$

$$L = 7 \mu\text{hy}$$

$$Q = 425$$

$$C_1 = 100 \mu\mu\text{f}$$

$$C_2 = 5 - 25 \mu\mu\text{f}$$

$$C_3 = 2 - 10 \mu\mu\text{f}$$

$$R = R_1 + R_2 = \frac{1}{r(\omega C)^2}$$

$$\omega L = \frac{2}{\omega C}$$

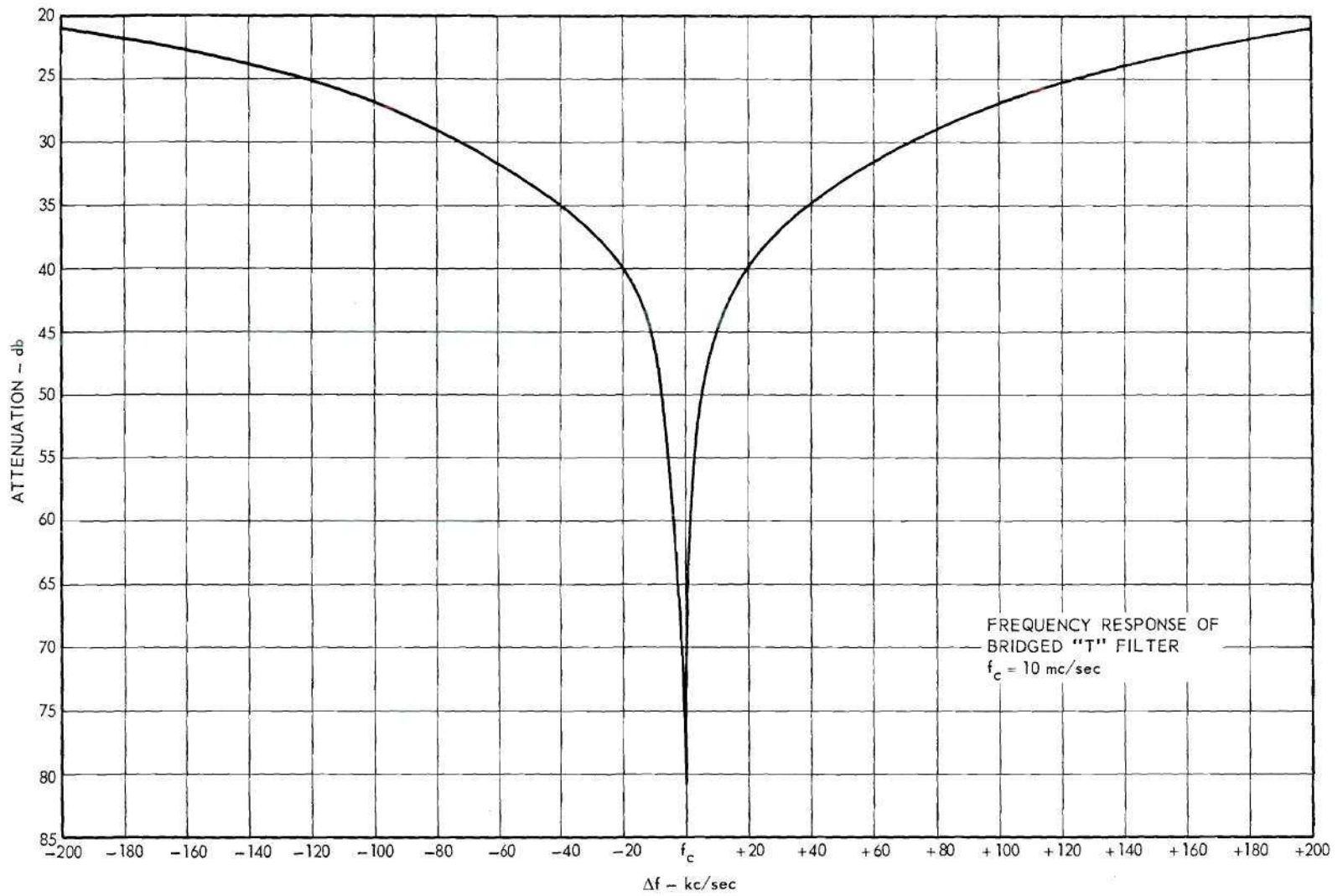
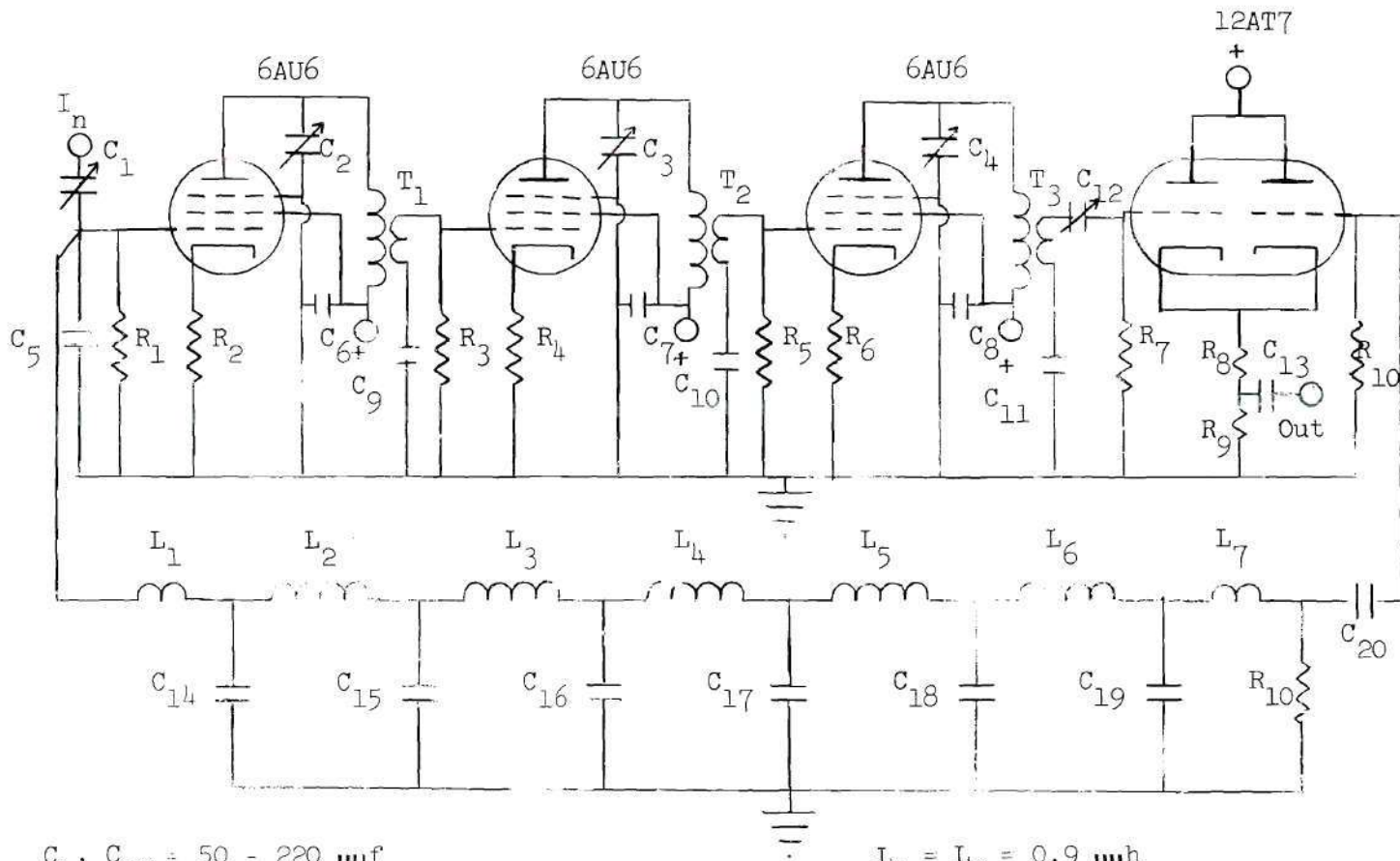


Figure 1B. Frequency Response of Bridged "T" Filter.



SCHEMATIC DIAGRAM OF CARRIER CANCELLATION DEVICE

APPENDIX C

- $C_1, C_{12} = 50 - 220 \mu\mu\text{f}$
- $C_2, C_3, C_4 = 0.7 - 30.0 \mu\mu\text{f}$
- $C_5 = 200 \mu\mu\text{f}$
- $C_6, C_7, C_8, C_{13} = 0.005 \mu\text{f}$
- $C_9, C_{10}, C_{11} = 5 \mu\mu\text{f}$
- $C_{14}, C_{15}, C_{16}, C_{17}, C_{18}, C_{19} = 550 \mu\mu\text{f}$
- $C_{20} = 0.05 \mu\text{f}$

- $L_1 = L_7 = 0.9 \mu\text{h}$
- $L_2, L_3, L_4, L_5, L_6 = 1.8 \mu\text{h}$
- $R_1, R_3, R_5, R_7, R_{10} = 470 \text{ K}$
- $R_2, R_4, R_6 = 5.6 \text{ K}$
- $R_8 = 18 \text{ K}$
- $R_9 = 100$
- $R_{10} = 50$

## BIBLIOGRAPHY

1. Lund, N., "Method of Measuring Adjacent Band Radiation from Radio Transmitters," Proceedings of the Institute of Radio Engineers, Vol. 39; pp 653-656; June 1951.
2. Hewlett Packard Instruction Manual, "Noise and Distortion Analyzer Model 330B/C," p II-8.
3. Firestone, W., and Magnuski, H., "Comparison of SSB and FM for VHF Mobile Service," Proceedings of the Institute of Radio Engineers, Vol. 44, pp 1834-1839; December 1956.
4. Guttwein, G. K., "High Frequency Crystal Filters," Proceedings of the Unclassified Sessions of Symposium on Electromagnetic Interference, p 289; November 1957.
5. Elec-Mechanics Company, "Bridged-T Technique for the Measurement of Spurious Radiation," Proceedings of the Armour Research Foundation Conference, p 264; December 1954.
6. General Ceramics Engineering Bulletin 21, Ferramic Toroid Selector For Design Engineers
7. Radio Corporation of America, Radiotron Designer's Handbook, p 328; 1953.
8. Ibid, p 320.
9. Milliman, J., and Taub, H., Pulse and Digital Circuits, McGraw-Hill Book Company, Inc., N. Y., 1956.